



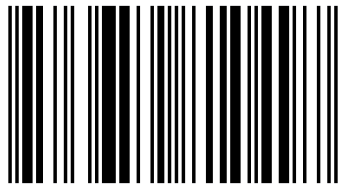
Structures in a changing climate highlights the effect of uncontrolled pollution, by human activities, on the environment. The book explains the processes leading to the corrosion of a typical steel structure subject to pollution from substances in the air, that arises from both natural and man-made pollutants. It is explained in two stages: Stage one where pollutants such as sulphur dioxide, carbon dioxide, chloride, etc are identified and quantified including their effect on materials. The reaction of the above air quality parameters with climate change parameters such as temperature, relative humidity, precipitation is analyzed through dose-response functions from several researchers, leading to the estimation of corrosion losses in steel structures. The second stage of the work used the estimated corrosion loss to determine their effect on a typical railway bridge loading in terms of moment of resistance and shear resistance. From the results, it is determined that overtime, increasing pollutant loading on the environment will cause failure of structures except this phenomenon is built into the design stage and carried out through proper maintenance.

Ben Ngene

Structures in a Changing Climate



Dr Ben. U. Ngene is from Ugwuaji Awkunanaw, Enugu. In 1988 graduated of Civil Engineering. He has varied industry experience up to managerial level and a double Master's and Ph.D holder in Structural and Water Resources Engineering. A COREN registered engineer. Dr. Ngene is currently involved in teaching and research at Covenant University, Ota.



978-3-659-81049-7

Ben Ngene

Structures in a Changing Climate

Ben Ngene

Structures in a Changing Climate

LAP LAMBERT Academic Publishing

Impressum / Imprint

Bibliografische Information der Deutschen Nationalbibliothek: Die Deutsche Nationalbibliothek verzeichnet diese Publikation in der Deutschen Nationalbibliografie; detaillierte bibliografische Daten sind im Internet über <http://dnb.d-nb.de> abrufbar.

Alle in diesem Buch genannten Marken und Produktnamen unterliegen warenzeichen-, marken- oder patentrechtlichem Schutz bzw. sind Warenzeichen oder eingetragene Warenzeichen der jeweiligen Inhaber. Die Wiedergabe von Marken, Produktnamen, Gebrauchsnamen, Handelsnamen, Warenbezeichnungen u.s.w. in diesem Werk berechtigt auch ohne besondere Kennzeichnung nicht zu der Annahme, dass solche Namen im Sinne der Warenzeichen- und Markenschutzgesetzgebung als frei zu betrachten wären und daher von jedermann benutzt werden dürften.

Bibliographic information published by the Deutsche Nationalbibliothek: The Deutsche Nationalbibliothek lists this publication in the Deutsche Nationalbibliografie; detailed bibliographic data are available in the Internet at <http://dnb.d-nb.de>.

Any brand names and product names mentioned in this book are subject to trademark, brand or patent protection and are trademarks or registered trademarks of their respective holders. The use of brand names, product names, common names, trade names, product descriptions etc. even without a particular marking in this work is in no way to be construed to mean that such names may be regarded as unrestricted in respect of trademark and brand protection legislation and could thus be used by anyone.

Coverbild / Cover image: www.ingimage.com

Verlag / Publisher:

LAP LAMBERT Academic Publishing

ist ein Imprint der / is a trademark of

OmniScriptum GmbH & Co. KG

Bahnhofstraße 28, 66111 Saarbrücken, Deutschland / Germany

Email: info@lap-publishing.com

Herstellung: siehe letzte Seite /

Printed at: see last page

ISBN: 978-3-659-81049-7

Copyright © 2016 OmniScriptum GmbH & Co. KG

Alle Rechte vorbehalten. / All rights reserved. Saarbrücken 2016

TABLE OF CONTENTS

Title Page		Page
Table of Contents	1
List of Figures	5
List of Table	6
List of Appendices	8

CHAPTER ONE: INTRODUCTION

1.1	Background of Study	9
1.2	Statement of Problem	10
1.3	Objective of Study	11
1.4	Significance of Study	11
1.5	Limitation of Climate and Pollution Data	12
1.6	Chapter Summary	12

CHAPTER TWO: REVIEW OF RELATED LITERATURE

2.1	Climate and Climate Change	13
2.2	Global Warming	14
2.3	Impact of Climate Change	15
2.3.1	Impact of Climate on Society	15
2.3.2	Impact of Human Being on Climate	17
2.3.3	Air Pollutants	17
2.3.4	Future of World Climate	18
2.4	Building Materials affected by Climate Change	19
2.4.1	Wood	19
2.4.2	Natural Stone	20

2.4.3	Masonry	21
2.4.4	Concrete	21
2.4.5	Weathering Steel...	22
2.5	Effect of Climate Change on Climate Parameters..							23
2.5.1	Temperature	23
2.5.2	Rainfall	24
2.5.3	Relative Humidity	25
2.5.4	Time of Wetness	25
2.6	Factors Affecting Air Quality	26
2.6.1	Sulphur Dioxide...	27
2.6.2	Smoke...	27
2.6.3	Oxides of Nitrogen...	27
2.6.4	Ozone	28
2.6.5	Carbon Dioxide	28
2.7	Dose Response Functions	32
2.7.1	Environmental Parameters.....	33
2.7.2	Estimation of Corrosion Losses	33
2.7.3	Impact Pathway...	35
2.8	Failure Probability of Corroded Structures	36
2.8.1	Reliability and Failure Probability...	37
2.8.2	Code Requirement for Reliability	38
2.8.3	Impart of Location of Structure and Corrosion...	38
2.9.	Chapter Summary	41

CHAPTER THREE: MATERIALS AND METHODS

3.1	Methodology	42
3.2	Data	42
3.3	Description of Study Area	46
3.4	Theory of Analysis	47

3.4.1 Mean of Pollutants and Climate Parameters ...	48
3.4.2 Standard Deviation	48
3.4.3 Variance	48
3.4.4 Coefficient of Variation	49
3.5 Effect of Analysis on Material... ..	49
3.5.1 Dose-Response Function and Estimation of Material Loss	49
3.5.2 BS EN ISO 9223:2012	52
3.5.2.1 Classification	52
3.5.2.2 Determination of Corrosion Rate... ..	56
3.5.2.3 Estimation of Corrosion Rate	58
3.6 Effect of Corrosion Loss on a Steel Bridge ...	58
3.6.1 Design of Simply Supported Railway Bridge... ..	58
3.6.1.1 Determination of loading... ..	58
3.6.1.2 Calculation of Moment and Shear Resistance... ..	59
3.6.1.3 Verification of Serviceability limit state of deflection... ..	59
3.6.2 Design Example	60
3.7 Chapter Summary	61

CHAPTER FOUR: RESULTS AND DISCUSSION

4.1 STAGE I – CLIMATE/CLIMATE CHANGE ...	62
4.1 Climate Change Predictions... ..	63
4.1.1 Emission Scenarios	64
4.1.2 Air Pollution and Climate... ..	66
4.2 Temperature	68
4.3 Relative Humidity	69
4.4 Sulphur Dioxide	69

4.5	Carbon Dioxide...	70
4.6	Air Quality Parameters – SO ₂ , NO ₂ , O ₃ , CO ₂	71
4.6.1	Estimation of Dose-Response Function	71
4.6.2	Analysis of Pollutants	78
4.6.2.1	Time Variation of parameters	80
4.6.2.2	Spatial Variation of thickness loss	84
4.6.2.3	Depth of Corrosion...	87
4.7	STAGE II – EFFECT ON STRUCTURE	90
4.8	Impact on a Railway Bridge Structure Used	91
4.9	Chapter Summary	110

CHAPTER FIVE SUMMARY AND CONCLUSIONS

5.1	Summary	111
5.2	Conclusions and Recommendation	112
5.3	Future Work	114
5.4	Reference	115
5.5	Appendix	125

LIST OF FIGURES

Figure 1.1 Typical U-Frame Railway Bridge showing atmospheric pollutants deposits	10
Figure 2.1 Steel Corrosion formations in anode reaction ...	23
Figure 2.2 Impact pathways for effect of acidic deposition in metals... ..	36
Figure 2.3 Loss of material on a typical I-beam section... ..	40
Figure 3.1 Map of study area, Guildford... ..	47
Figure 3.2 Classification of atmospheric corrosivity... ..	53
Figure 3.3 Half through Bridge structure and component.....	61
Figure 4.1 Scenarios for GHG emissions from 2000 to 2100	64
Figure 4.2 Temperature change with time as a result of increase in greenhouse gases	68
Figure 4.3 Reduction in Relative Humidity with time	69
Figure 4.4 Sulphur dioxide reductions with time... ..	70
Figure 4.5 Extract of Carbon dioxide emission by fuel sources in 2010... ..	71
Figure 4.6 Projected increase in Carbon dioxide concentration with time... ..	71
Figure 4.7 Comparison of the dose-response functions from Various researchers and the average dose-response function.	74
Figure 4.8 Average corrosion rate against time... ..	77
Figure 4.9 Difference in mean against various pollutant parameter changes.....	80
Figure 4.10 Increase in SO ₂ with percentage increase.	81
Figure 4.11 Increase in Temperature with percentage	

increase.81
Figure 4.12 Increase in Relative Humidity with percentage increase...	...81
Figure 4.13 Increase in thickness loss with SO ₂ increase...	82
Figure 4.14 Decrease in thickness loss with increase in temperature...	...82
Figure 4.15 Increase in thickness loss due to increase in relative humidity...	...83
Figure 4.16 Corrosion rate for rural environment...	...86
Figure 4.17 Corrosion rate for urban environment...	...86
Figure 4.18 Corrosion rate for Industrial environment...	... 87
Figure 4.19 Cross-section arrangement of the bridge...	... 91
Figure 4.20 Track position for the girder...	...93
Figure 4.21 Girder section properties...	... 94
Figure 4.22 Effect of thickness loss on moment resistance of bridge girder...	...108
Figure 4.23 Effect of thickness loss on shear resistance of bridge girder...	...108
Figure 4.24 Effect of thickness loss on deflection of bridge girder...	...109

LIST OF TABLES

Table 2.1 Unsheltered concentrations of some important pollutants in different types of environment	29
Table 3.1 Climate and pollution data used for the dose-response function..	44
Table 3.2 Categories of corrosivity of the atmosphere...	... 54

Table 3.3	Corrosion rate for first year exposure under various corrosivity categories	56
Table 4.1	Projected global average surface warming and sea level rise at the end of 21 st Century...	66
Table 4.2	Mean value of parameters from differing time period...	67
Table 4.3	Determination of mass loss based on several dose-response functions	73
Table 4.4	Mass loss based on several dose-response functions and an average dose-response...	74
Table 4.5	Annual max/min corrosion rate with the average Corrosion based on all the dose-response functions.....	77
Table 4.6	Classification of mass loss according to ISO standard	78
Table 4.7	Calculation of thickness loss against time...	79
Table 4.8	Effect of percentage change on parameters relative to 2050 values	80
Table 4.9	Rural values of SO ₂ (2<SO ₂ <15)	84
Table 4.10	Urban values of SO ₂ (5<SO ₂ <100)	85
Table 4.11	Industrial values of SO ₂ (50<SO ₂ <400)	85
Table 4.12	Depth of corrosion penetration for various environments...	93
Table 4.13	Thickness losses analyzed...	100
Table 4.14	Calculated resistance for various corrosion types	107

LIST OF APPENDICES

Appendix A	Definition of Terms... ..	125
Appendix B1	Estimate of mean values of parameters using pre-industrial revolution records...	126
Appendix B2	Estimate of mean values of parameters using industrial revolution records	127
Appendix B3	Estimate of mean values of parameters using after-industrial revolution records ...	129
Appendix B4	Estimate of mean values of parameters using future projection records	130

CHAPTER ONE

INTRODUCTION

1.1 BACKGROUND OF STUDY

“Then the Lord rained down burning sulphur on Sodom..... out of the heavens”. Gen. 19:24, NIV Bible (2005). Does the situation of the current climate reflect this quote? What can be done to ensure that similar disaster does not affect the universe?

Deterioration of materials due to air pollution come at high cost and the damage pose a long term effect on available infrastructure provided at high cost to the economy of the nation. Duke (2011) writing in this shrinking land, climate change and Britain coasts notes that “The oceans are the grave yards of the lands. Lands became eaten away by the action of the seas, and it is no surprise to find that most of the world’s shorelines are in a state of erosion. The fringes of Britain, its cliffs and beaches are shrinking, disappearing into the surrounding sea because of coastal flooding, erosion and land sliding. Is climate change speeding up the process; are our homes, our villages and towns, at risk?” the author asked. Feenstra (1984) has observed that “the effect of atmospheric pollutions on building is the best evidence of the examples of damages related to the heating of fossil fuels. The pollution form of damage to buildings is seen in discoloration, failure of protective coating, loss of details in carvings and structural failure”. In this regard, it is important to observe that the rate of this damage has increased greatly since the industrial revolution. While much work on the effect of climate change has centered on coastal erosions,

marine infrastructure, building and cultural artifacts, more need to be done on many steel bridges and other railway infrastructures which dot the nation's highways and rail lines.

Dose-Response approach was used to determine the rate of corrosion of a road steel bridge with rail line at grade, located in Guildford (see figure 1.1) while determining its load carrying capacity over time.



Fig 1.1 Typical U-Frame Railway Bridge showing atmospheric pollutant deposits arrowed.

1.2 STATEMENT OF PROBLEM

As noted by Ayoade (2004), it is now increasingly clear that man is capable of inadvertently influencing global climate through anthropogenic heat production and the emission of green-house gases. Despite quite extensive experimental test programme, such as the assessment of global warming damages by Extern E (1998) project, the prediction of the likely corrosion loss of materials is still

rather low, even though the various factors that influence atmospheric corrosion are known.

The effect of such loss on structure in place need to be further studied to engender better understanding of structural failure possibilities or its reliability.

1.3 OBJECTIVE OF STUDY

The objectives of this study are therefore summarized as follows:

- i. Determine the Dose-Response model of weathering steel in UK using weather parameters for London.
- ii. Estimate the deterioration of a steel bridge in Guildford over time using the dose-response function approach.
- iii. Calculate the resistance of a steel bridge structure over time subject to such deterioration.
- iv. The general objective of this research is to study the factors that actually have impact on the service life existence and progress of deterioration of structures exposed to atmospheric weathering.

1.4 SIGNIFICANCE OF STUDY

Structural failure as a result of pollutant exposure does not occur unless where there is wrong design of the structure or the owner has not carried out routine maintenance.

However, valuation of material damage is complex for a number of reasons which include material type and the nature and importance of the object. Cost of replacement and maintenance can be easily determined provided that there are clear guidelines as to what action should be taken and at what time, example replacement of

steel member when a given depth of material has corroded, Extern E (1998).

This study therefore tries to understand how air quality affects the corrosion of materials of construction especially steel in unsheltered condition.

1.5 LIMITATION OF CLIMATE AND POLLUTION DATA

Numeric determination of climate and pollution parameters is required to calculate the deterioration rates for steel in London over time. According to Brimblecombe et al (2008) it is important to note that there is the need for caution in the use of long term millennium data that involve historic, non-instrument and instrument records for future predictions as they are inhomogeneous.

Data used in this work being a secondary data obtained from the reference above need to be treated with caution. The reliability of the data will be improved upon with future information as they occur. For the Dose-Response function, the work utilized the already determined functions by Kucera et al., (2005) for the Multi-Assess project in multi-pollutant exposure case and further work done on the subject by Mikhailov (2001) and ISO 9223 (2012) etc.

1.6 CHAPTER SUMMARY

This chapter introduced the subject of impact of climate change on the rate of deterioration of existing structures. It also looked at the significance and objective of the study while noting past research on the subject. Detailed literature review to determine what is known and any gap in knowledge will therefore follow.

CHAPTER TWO

REVIEW OF RELATED LITERATURE

2.1 CLIMATE AND CLIMATE CHANGE

Climate is a term used widely to describe the “average weather” for a given region over decades or more or being used to refer to condition across the entire planet. The nature of the earth’s climate at both the regional and global scale is the result of an interconnected system driven by the uneven heating of the planet by solar radiation. This system transfers heat from low to high latitudes, and involves all the Earth’s sphere: the atmosphere, hydrosphere (mainly the ocean), cryosphere, biosphere and lithosphere. It tends to keep the Earth’s radiation budget in balance globally so that, incoming radiation is equaled by outgoing radiation (Wilson et al., 2001).

The climate in any given region involves both the average of the weather and the typical extent to which condition followed from the average. “The term ‘weather’ refers to the daily changes in the state of the atmosphere at a specific location. Climate involves variables such as temperatures, humidity, windiness, cloudiness and precipitation” (Danny Harvey, 2000). Climate is much more than the atmospheric variables, but depends on all other components that interact together to form part of the climate system. This made climate system study wide ranging and multi-disciplinary viz Meteorology, Physical and Chemical Oceanography, Atmospheric and Soil chemistry, Cloud and Aerosol Physics, Marine and Territorial Ecology and Engineering. In recent years media attention

has focused on changing world climate and the impacts on the human experience, this may cause (Hart, 2000). Research has shown that the climate is changing globally, with the world being about 0.6°C warmer than one hundred year ago (Hulme & Jenkins., 1998). “The warmest year ever recorded have been (in increasing order) 1990, 1995, 1997 and 1999; the last year 2010 being the warmest since about 1204” (Lamb, 1995). In the United Kingdom, five of the six warmest years in the 340 year Central England Temperature series occurred since 1988. Several researches from sources estimate possible rate of global warming over the next century to range from “0.16°C per decade to 0.35°C per decade. In the same period global sea-level is predicted to rise from between 2.4cm per decade to 10.0cm per decade” (Hart, 1997).

2.2 Global Warming

The term “greenhouse effect” is used to describe the tendency of the atmosphere to create a warmer climate than would otherwise be the case (Danny Harvey, 2000). When radiation hits a surface or a gas molecule, it loses energy which causes the wave length of that radiation to lengthen (Wellburn, 1994). Earth’s surface warming, either by solar radiation or by re-radiated infrared (IR) causes evaporation of water and upward convection of air, both of which transfer energy from the Earth’s surface back into the atmosphere.

According to Ayoade (2004), the near consistent increase in the Earth’s temperature since 1970s has been explained by two factors. The first is the increase in anthropogenic heat production as a result of increase in urbanization and industrial activities worldwide. The

second and more important factor is the increase in the generation of greenhouse gases such as CO₂, methane, nitrous oxide and chlorofluorocarbons (CFCs) by various human activities especially transportation and manufacturing activities. It is estimated that CO₂ and CFCs account for about 80% of global warming. These and other greenhouse gases absorb infrared terrestrial radiation preventing it from escaping to space thus warming the earth's atmosphere. It is estimated that if the present rate of increase in CO₂ in the atmosphere continues, it will be 450ppm in 2050 and between 500 and 600ppm in 2075.

2.3 IMPACT OF CLIMATE CHANGE

Climate influences man in diverse ways. Man in turn influences climate through his various activities such as in industry and manufacturing, transportation and burning of coal and other fossil fuels (Ayoade, 2004).

2.3.1IMPACT OF CLIMATE ON SOCIETY

Changes in climate exert a lot of influence on human beings and the degree to which a particular environment is exposed to damage by climate reasons is termed its vulnerability. The human nature to adapt and withstand adverse climate impacts, however, is termed its resistance.

Studies have indicated that the ability of society to withstand adverse climate is not a linear function of its wealth or degree of development (Burton et al., 1978). As observed by (Critchfield, 1974) energy, human health and comfort are more susceptible to be affected by climate than any other factor in the physical

environment. Example, though ultraviolet rays help to form vitamin D in the skin and devitalize bacteria and germs, they can also cause sunburn and inflammation of the skin. In fact, ultraviolet rays coupled with intense heat can cause cataract of the eye. On the positive side also, fresh air, mild temperature, moderate relative humidity and sunshine also have healing value.

Economic activities such as in manufacturing industry, commerce, utilities, agriculture and animal husbandry, transport and communication are all influenced to varying degree by climate. These human economic activities can only be successfully pursued under right climate conditions (Mather, 1974; Smith, 1975, Hobbs, 1980)

Climate also influences the way a house is built and the type of dress humans wear and they vary from culture to culture and from climate zone to another. In this regard, (Griffiths, 1976) has noted the classification of the world into zones with respect to their clothing requirements to meet normal human body heat balance. Building location, materials choice, designs and method of air-conditioning of structure is affected by climate and weather conditions. In addition, however, the building structural safety and ability to carry the stresses arising from the prevailing climate during its anticipated lifetime must be guaranteed (Smith, 1974; Critchfield, 1974).

Since construction activities take place in outdoor conditions, current weather condition with regard to rain, flood, snow, high winds, and temperature extremes can affect it adversely. Estimates of the number of workable days for construction purposes are made using information on the weather variables (Smith, 1975).

2.3.2 IMPACT OF HUMAN BEING ON CLIMATE

Examples of attempts to control weather by human include seeding to augment precipitation or suppress hail or lightning or to clear fog or modify the structure and movement of hurricanes.

Man may also influence climate inadvertently through his various actions and activities such as urbanization and industrialization, oil drilling activities, falling of trees, farming activities, draining of marshes or creation of artificial lake when rivers are dammed to provide water for various uses or for generation of hydroelectric power.

The greatest impact of man on climate is evident in urban areas. Here, the actions of man have such a tremendous impact on climate that the climate prevailing in urban areas is quite distinct in character from that in the surrounding rural areas (Ayoade, 2004). This point is clearly seen in the results achieved by this work where the corrosion in the urban/Industrial area is higher than for a rural area by a factor of between 2 and 3 respectively.

According to (WMO, 1965) the balance between the sources from which pollutants arise and the factors favourable to their dilution and dispersal within the atmosphere determine whether or not a pollutant will constitute a hazard to human health and welfare.

2.3.3 AIR POLLUTANTS

Either by natural or man-made process, the release of substances that are not of natural origin into the air from other sources is termed air pollution.

Buildings are affected by corrosions due to air pollution, metals are oxidized and there is deterioration of plants. In the United States alone, property damage due to air pollution is estimated to be over \$10.0 billion a year while damage to crop alone amounts to over \$500 million a year (Maunder, 1970).

Research has also shown that in Great Britain, the larger the city the higher the incidence of bronchitis-emphysema (McDermoll, 1961). Other disease associated with air pollution includes influenza, lung cancer, asthma and pulmonary heart disease.

Working hand in hand with meteorologists, urban planners can contribute to air pollution control through proper urban design, involving zoning, proper land use planning and site selection as well as the use of green areas and buffer zones (Bach, 1972).

2.3.4 FUTURE OF WORLD CLIMATE

According to the SMIC report (1971), past land use from their natural vegetation to pasture and for agricultural purposes has affected the climate though not by choice.

The modification of the natural vegetation has affected several important climate parameters such as surface roughness as well as the hydrological properties of the surface (Lockwood, 1979).

According to Barry and Chorley (1976), were it not for the removal of CO₂ from the air by the land biosphere and the oceans, the increase of the pollutant in the atmosphere would have been about 20%.

Studies such as those carried out at the Hadley Centre (SCOPAC, 2001) predict that in Southern England:

- It will continue to get warmer
- Rainfall will continue to increase in winter and decrease in the summer, but with an overall increase in both total and effective rainfall.
- Sea level will continue to rise
- There is also the possibility of higher number of extreme weather, rainfall and storm events.

Essentially, these predictions would appear to be continuation of current trends but with expected increased rate of change.

Finally, human's Engineering skills and ability to deploy his technological capability is required now and in the future as it grapples with the challenges of ensuring that it does not live at the mercy of the climate.

2.4 BUILDING MATERIALS AFFECT BY CLIMATE CHANGE

As the climate change, man-made response to overcome the earth is affected in many ways, such as in:

2.4.1 WOOD

In many Engineering structures, such as building, railway and bridge structures, wood form part of the materials exposed to the environment. Direct atmospheric pollution does not however affect wood as much as the problem caused by water and humidity. Uncontrolled variations of relative humidity in the environment and precipitation are the principal hazard to the preservation of wood in and outdoors (Kozłowski, 2007).

Woods are complex materials and they differ greatly in their porosity and water resistance. Example is the hard wood, though few of them can withstand outdoor exposure without protection. A greater bulk of exposed wood, such as softwood, if left unprotected would become water logged and develop excessive porosity through bacterial action or rot (Banks and Evans., 1984). The use of wood as a construction material saves a lot of energy and hence helps to reduce global warming. However, cutting down of trees to form timber for construction also contributes to global warming by reducing the amount of oxygen regenerating plants in earth natural system.

Timber shrinks with change in moisture content especially under unsheltered condition. BS 5268-2 and Eurocode 5 indicate three types of service class of wood in use to include:

Service Class 1 for moisture content at 20°C and relative humidity of 65% per annum. Service Class 2 is for moisture content at 20°C and relative humidity of 85% per year and Service Class 3 is used to indicate wet condition at temperature and relative humidity greater than Class 3 (Ozelton et al., 2008).

Class 3 is used for fully exposed timber under external use and creep deflection of beams in this category can be affected by method of drying and loading condition.

2.4.2 NATURAL STONE

Serious attack on natural stone by atmospheric pollutants is confined to limestone and calcareous sandstones (UKBERG, 1990). It has been observed that stone, particularly granite, are not

seriously affected by pollution. Stone damage problems are also known to occur through frost damage or by crystallization of soluble salts. The occurrence of weathering of stone is mainly due to carbon dioxide present in the atmosphere.

According to (Cooke and Gibbs, 1994), CO₂ dissolves in rain-water, producing an acidic solution. The acidic rain-water reacts with calcium carbonate in the stone to form soluble calcium bicarbonate. In the presence of SO₂, the rain-water acidity increases and a much faster chemical attack occurs.

2.4.3 MASONRY

Research by (UKBERG, 1990) has shown that there is low evidence of damage to brickwork by industrial pollutants. Bricks are noted to be stable without protection except when damaged by frost acts. Renderings are also not adversely affected by acid pollutants but a substrate can be affected by sulphate action.

2.4.4 CONCRETE

The main binding material for concrete is Portland cement, an alkaline material subject to acid attack. The damage to concrete as a result of climate impart may be in the form of spalling, surface erosion and corrosion of embedded steel. Apart from surface erosion, damage to concrete may likely be in form of natural carbonation and ingress of chloride ions as against interaction with pollutants such as SO₂ (Etern E, 1998a).

Corrosion of embedded steel reinforcement in concrete affects its durability. The alkaline nature of the cementitious concrete protects

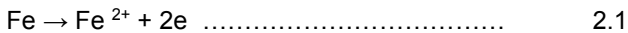
the reinforcement from corrosion. Expose of concrete to air and rain over a period of years neutralizes the alkalinity, causing the pH of the cement paste to fall and leaving the steel open to corrosion (UKBERG, 1990). The interactions of CO₂ and SO₂ in the atmosphere with calcium hydroxide of the cement Paste bring about the neutralization of the pH (Lahdensivu et al., 2009).

2.4.5 WEATHERING (CARBON) STEEL

Carbon steel is high strength, low alloy weldable structural material which possesses good weather resistance in many atmospheric conditions with minimal need for protective coatings (The Steel Construction Institute, 2003). Weathering steel contains alloying elements such as Nickel, Copper, Phosphorus and Chromium (SCI, 2006; Kihira et al., 2005).

Additional thickness is added to steel, which is outside the calculated section resistance, to take care of the slow rusting overtime in unpainted weathering steel. This additional thickness is dependent on prevailing atmospheric condition as determined in clause 4.5.6 of BS 5400-3; 2000.

Metals atmospheric corrosion is achieved by electrochemical process, which takes place in corrosion cells with anodes and cathodes as shown in figure 2.1.



Anode Reaction: $2\text{Fe} \rightarrow 2\text{Fe}^{2+} + 4\text{e}^-$

Cathode Reaction: $\text{O}_2 + 2\text{H}_2\text{O} + 4\text{e}^- \rightarrow 4\text{OH}^-$

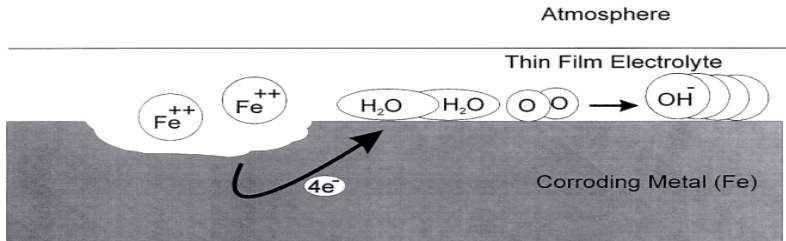


Figure 2.1 Steel corrosion formations in anode reaction according to Etern E, 1998a

A wet electrolyte is needed for atmospheric corrosion. This is enhanced by such climatic parameters as precipitation, humidity, temperature and degree of atmospheric pollutants. Sulphur dioxide causes most damage, of all the atmospheric pollutants, while in coastal regions chlorides also play a considerable role (EternE, 1998a).

The role of NO_x and ozone in the corrosion process of metals is not yet fully understood, though there is evidence (Kucera, 1994) to suggest that ozone play a significant role in quickening some reactions.

2.5 EFFECT OF CLIMATE CHANGE ON CLIMATE PARAMETERS

2.5.1 TEMPERATURE

The world temperature is predicted to rise over the next century. This increase of some few degrees will be critical to many

aspects of our lives and the health of ecosystems and agriculture (Brimblecombe et al., 2007).

By definition the degree of hotness of a body as measured by a thermometer is its temperature. One critical aspect of temperature that affects large structures is seasonal changes. Large seasonal changes in temperature impose greater stress on buildings and structures. The temperature data for this work is based on Central England Temperature Record (CETR) with modification for past records, shown in Table 3.1 below (Brimblecombe et al., 2008; Manley, 1974; Parker and Horton, 2005; Parker et al., 1992). Generally, studies have shown that temperature have correlation with corrosion rates (ECE, 1984). Temperature is noted to increase the rate of reaction, though for steel the rate decrease with increase in temperature and it also dries the surface.

2.5.2 RAINFALL

Corrosion of metals by rainfall is dependent on the pH of the rain, intensity, duration and amount. Though rainfall acidity is not easy to estimate, it is known from twentieth century measurements and records to be low (Brimblecombe et al., 2008). Coal ash present in the past century tended to make rainfall alkaline, hence a pH value of 5.5 is used for this work as in table 3.1.

The presence of SO₂ decreases the pH of rain, and causes faster chemical attack. This can occur by the dissolution from rain acidity or attack of dry deposition of pollutant. As reported in (Wang et al., 1997, Misawa et al., 1974), “hygroscopic SO₂ in the industrial atmosphere often lowers the pH of water, wets rust layer and

dissolves the initial corrosion products of γ -FeOOH, and also promotes the phase transformation of γ -FeOOH to amorphous ferric oxyhydroxide and α -FeOOH". This transformation for weathering steel is known to take place within the first three years of exposure.

2.5.3 RELATIVE HUMIDITY

Relative humidity is one of the climate parameters included in most of the established dose-response functions. It defines the percentage of vapour density to saturation vapour density at any given time. For relative humidity, the transformed variable is $Rh_{60} = (Rh-60)$ when $Rh > 60$; otherwise 0 is used in the dose-response function (Kucera, 2007).

As indicated by Brimblecombe et al., (2007) cycles of relative humidity causes crystallization and dissolution, which exert stress on structural materials in which weathering salts are present, Arroyave et al (1995); Henriksen and Rode (1986) concluded that at high relative humidity, SO_2 might form ferrous sulphate, which would attract water and be dissolved on steel surfaces, thereby accelerating the corrosion with little contribution from NO_2 .

2.5.4 TIME OF WETNESS

For weathering steel, the time of wetness (TOW) may be interchangeably used with relative humidity. This is because steel show high critical humidity for corrosion process (Leuenberger-Minger et al., 2002).

Bartonj and Cherny (1980) has shown that there is a correlation existing between corrosion under absorbed water films and the

amount of SO₂ absorbed by the films over a period equal to TOW as in

$$f_{\text{dry}} = C [\text{SO}_2]^A \cdot \text{TOW}^B \dots\dots\dots 2.2$$

The power functions take into consideration the nonlinearity of this expression regarding both SO₂ and TOW.

The deposition of atmospheric pollutants such as sulphate dioxide on outdoor structures such as buildings and bridges is influenced by time of wetness or humid condition. Water soluble gases such as SO₂ and other particulate matters can be deposited more effectively under humid environment than in dry condition.

2.6 FACTORS AFFECTING AIR QUALITY

Chemical composition of the atmosphere is of great importance to the corrosion process because of their thermodynamic and kinetic effect on corroding material. By thermodynamics, we look at the effect of heat in changing the physical and chemical processes of the material. Thermodynamics therefore defines how stable the material will be under the inherently prevailing conditions of the environment. Kinetic effect on the other hand affects the rate of oxidation of a metallic material in an environment. Mellanby (1988) observed that the most important pollutant that affects structural materials are sulphur dioxide and oxides of nitrogen and their oxidation products, together with chlorides and particulate matter. Ozone was also considered as its presence affects the quality of the air.

2.6.1 SULPHUR DIOXIDE

Emission of this substance arises from man's activities such as in different fuel use. The observed decline in United Kingdom of SO₂ emissions since 1980 has been attributed to equal proportions to energy economies, reduction in sulphur content of fuels, changes in fuel use patterns (e.g. to natural gas) and industrial modernisation.

Results of site monitoring have revealed that over the past 30 years, the decrease in urban SO₂ concentrations have clearly arisen primarily from the decrease in domestic and industrial/commercial emissions (Mellanby – 1988)



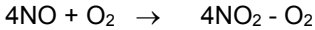
2.6.2 SMOKE

While the current United Kingdom average smoke concentration of urban annual means is 17µgm⁻³, that of central London is put at between 25-35µgm⁻³. This represent a fall from the 1960 average of 140µgm⁻³ with some areas as high as 350µgm⁻³. The consequence is that motor, especially, diesel vehicles are often the predominant contributor to smoke concentration.

2.6.3 OXIDES OF NITROGEN

Estimates from Warren Spring laboratory (UKBERG, 1990) indicates that United Kingdom annual emission of NO_x was almost flat from 1905 to 1945 but increased by a factor of 2 to date. This increase is attributed to increased oil consumption by the transport sector. Peak hourly concentration are affected by meteorological

conditions and for long it is put at an average of $60-80\mu\text{gm}^{-3}$ for NO_2 and $40 - 65\mu\text{gm}^{-3}$ for NO



2.6.4 OZONE

These are not considered as primary pollutants. It is produced in high concentrations in the stratosphere by UV irradiation and transported into the free troposphere to supplement ozone produced there photo chemically (UKBERG, 1990). For the United Kingdom, the average annual concentration in urban areas range from $20-40\mu\text{gm}^{-3}$ while for rural area it is $40-60\mu\text{gm}^{-3}$. For reason of area of primary production, ozone depends on meteorological variation for its dispersal. Apart from that, it also depends on sufficient sunlight and favourable air mass trajectory to transport it from source to its receptors. Hydrocarbons in the atmosphere can be oxidized by ozone as follows:



2.6.5 CARBON DIOXIDE

This is not considered as pollutant gas. However, its presence in the air does add to the acidity of rain water and thereby cause some degradation to limestone and concrete. Combustion of fossil fuels has caused a considerable increase in atmosphere concentration of CO_2 from approximately 290ppm in 1870 to 340 in 1985 (Brimblecombe, 1986). As a result, attacks by CO_2 on calcareous stones proceeds more rapidly because the CO_2

concentration increase leading to a higher partial pressure and more decay and directly because of the low pH (UKBERG, 1990).

Table 2.1 show unsheltered concentration of some important pollutant in different types of environment according to BS EN ISO 9223 (2012)

Pollutant	Concentration/deposition (yearly average value)	Source
SO ₂	rural: 2 – 15 (µg/m ³) urban: 5 – 100 (µg/m ³) industrial: 50 – 400 (µg/m ³)	The main sources for SO ₂ are the use of coal, oil and emissions from industrial plants.
NO ₂	rural: 2 – 25 (µg/m ³) urban: 20 – 150 (µg/m ³)	Traffic is the main source for NO ₂ emissions.
HNO ₃	rural: 0,1 – 0,7 (µg/m ³) urban/industrial: 0,5 – 4 (µg/m ³)	HNO ₃ is correlated with NO ₂ . High concentrations of NO ₂ , organic compounds and UV light increase the concentration.
O ₃	20 – 90 (µg/m ³)	O ₃ is formed in the atmosphere by an

		interactions among sunlight, oxygen and pollutants. The concentrations are higher in polluted rural atmospheres and lower in high-traffic urban areas.
H ₂ S	normally: 1 – 5 (µg/m ³) industrial and animal shelter: 20 – 250 (µg/m ³)	There are some natural sources, for instance swamps and volcanic activities. The pulp and paper industry and farming give the highest concentrations.
Cl ₂	normally: 0,1 (µg/m ³) some industry plants: up to 20 (µg/m ³)	The main source is emissions from the pulp and paper industry.
Cl ⁻	0,1 – 200 (µg/m ³) depending on geographic situation –	The main sources are the ocean and de-icing of roads.

	in marine atmospheres 300 – 1 500 ($\mu\text{g}/\text{m}^3$)	
NH_3	normally low concentrations: < 20 ($\mu\text{g}/\text{m}^3$) close to source: up to 3 000 ($\mu\text{g}/\text{m}^3$)	Fertilization in the agricultural area source and emissions from industry and food production can give the highest average values.
Particles- PM_{10}	rural: 10 – 25 ($\mu\text{g}/\text{m}^3$) urban/industrial: 30 – 70 ($\mu\text{g}/\text{m}^3$)	Rural: largely inert components Urban: high-concentration traffic areas, corrosive components Industrial: emissions from production can give high concentrations.
Particles (dust deposits)	rural 450 – 1 500 [$\text{mg}/(\text{m}^2.\text{a})$] urban/industrial: 1 000 – 6 000 [$\text{mg}/(\text{m}^2.\text{a})$]	Rural: largely inert components Urban and

		industrial: corrosion active components (SO ₄ ²⁻ , NO ₃ ⁻ , Cl ⁻)
Soot	rural: < 5 [mg/(m ² ·a)] urban and industrial: up to 75 [mg/(m ² ·a)]	Coal and wood burning is a major source. Diesel soot from cars is another source.

NOTE: This table introduces general limits of concentrations or deposition of pollutants. The real (actual) intervals are different in the particular parts of the world, depending on the level of industrialization and the application of measures for the abatement of pollution (legal measures, end-of-pipe technologies, etc.).

2.7 DOSE – RESPONSE FUNCTIONS

Literally, this is the function that determines the impact of the application of a certain quantity of a substance on the receptor. For air pollution the dose-response function is usually stated directly in terms of prevailing ambient concentration, hence the term exposure-response (E-R) function is sometimes used to describe the function according to EternE. Environmental impacts of dose response functions are liberally considered as measured data are globally used to predict equation on local scale. In this regard, dose-response functions are geographically transferable.

2.7.1 ENVIRONMENTAL PARAMETERS:

Dose-response functions include such climate data as temperature (T), relative air humidity (Rh), gaseous emissions in the air (SO₂, NO₂ and O₃) and amount of precipitation. Difficulty in obtaining time of wetness (TOW) resulted in its exclusion (Mikhailov, 2001).

Though polluting gaseous emissions such as SO₂, NO₂ and O₃ were included in the statistical analysis, the negative correlation between NO₂ and O₃ (NO₂ level is low in rural and high in urban atmosphere, while O₃ is the reverse) is observed. Note that it is difficult to identify the effect of NO₂ and O₃ separately. See paragraph 2.6.3.

2.7.2 ESTIMATION OF CORROSION LOSSES

The additive corrosion losses k in terms of f_{dry} and wet f_{wet} precipitates is considered (Mikhailov, 2001):

$$K = f_{dry} \cdot t^k + f_{wet} t^m \dots\dots\dots 2.6$$

$$K = f_{dry} (T, Rh, [SO_2], [O_3]) \cdot t^k + f_{wet} (Rain, [H^+]) t^m \dots\dots 2.7$$

where t is time, and k and m are constants and

$$f_{dry} = c [SO_2]^A TOW^B \text{ as earlier noted in equation .}$$

The term f_{wet} describes the effect of precipitates and their acidity.

$$f_{wet} = C_H (Rain, [H^+]) \dots\dots\dots 2.8$$

where C_H is a constant, Rain is the amount of precipitates and [H⁺] is the concentration of hydrogen ions in the precipitate. C_H value can be negative (washing effect) or positive.

The effect of chlorides in precipitates on f_{wet} is expressed similarly.

$$f_{wet} = C_{CL} Rain [CL^-] \dots\dots\dots 2.9$$

where C_{CL} is a constant, and [CL⁻] is the concentration of chloride in the precipitates. Chloride effect is however noted for marine

(coastal) environment. The corrosion loss equation is nonlinear hence the use of nonlinear regression analysis method.

Many researchers have tried fixing a general function for dose-response that relates to all environmental parameters. Meteorological and site differences have however limited their success. A listing of some of these function considered in this work is as follows:

Lipfert (1987) gives annual loss for unsheltered zinc:

$$M_L = [t^{0.78} + 0.46 \log_e (H^+)].[4.24 + 0.55Fe_2.SO_2 + 0.29Cl^- + 0.029H^+] \dots \dots \dots 2.10$$

Zinc though not an important construction material is used in steel coating as in galvanization. Its low corrosion rate and preference to the substrate recommend it as protective coating.

Butlin et al (1992) suggested for unsheltered zinc in one year loss as

$$ER = 1.38 + 0.038SO_2 + 0.48p \dots \dots \dots 2.11$$

This function has been revised by Kucera (1994) to include ozone and time of wetness terms

$$ML = 14.5 + 0.043.TOW. SO_2.O_3 + 0.08.H^+ \dots \dots \dots 2.12$$

For the multi-Assess exposure, Kucera (2005) used for the carbon steel the dose-response function as

$$ML = 29.1 + \{21.8 + 1.38[SO_2]^{0.6}Rh_{60}e^{f(T)} + 1.29 Rain[H^+] + 0.589Pm_{10}\}t^{0.6} \dots \dots \dots 2.13$$

Weathering steel, an alloy of Nickel, Copper etc. has the dose-response function as shown for outdoor application (Mikhailov, 2001).

$$\ln(\text{ML}) = 3.54 + 0.33 \ln(t) + 0.13 \ln(\text{SO}_2) + 0.020\text{Rh} + 0.059(\text{T}-10)$$

for $T \leq 10^\circ\text{C}$ 2.14

and

$$\ln(\text{ML}) = 3.54 + 0.33 \ln(t) + 0.13 \ln(\text{SO}_2) + 0.020\text{Rh} - 0.036(\text{T}-10)$$

for $T > 10^\circ\text{C}$ 2.15

where t = time in years, T = Air temperature, Rh = Relative humidity (%), $[\text{SO}_2]$ = SO_2 concentration ($\mu\text{g}/\text{m}^3$), $[\text{NO}_2]$ = NO_2 concentration ($\mu\text{g}/\text{m}^3$), O_3 = O_3 concentration ($\mu\text{g}/\text{m}^3$), Rain = Quantity of Rainfall (mm), $[\text{H}^+]$ = H^+ concentration (mg/L) and $[\text{CL}^-]$ = CL^- concentration (mg/L).

2.7.3 IMPACT PATHWAY

The EternE (1998a) project identified metals (steel) as one of the pathways of acidic emissions and precursors of photo-oxidants effect on materials. The impact pathway follows the following routes: discoloration, materials loss and structural failure. Structural failure from pollutant exposure is more noticeable where there is fundamental flaw in design or the property does not have good routine maintenance programme.

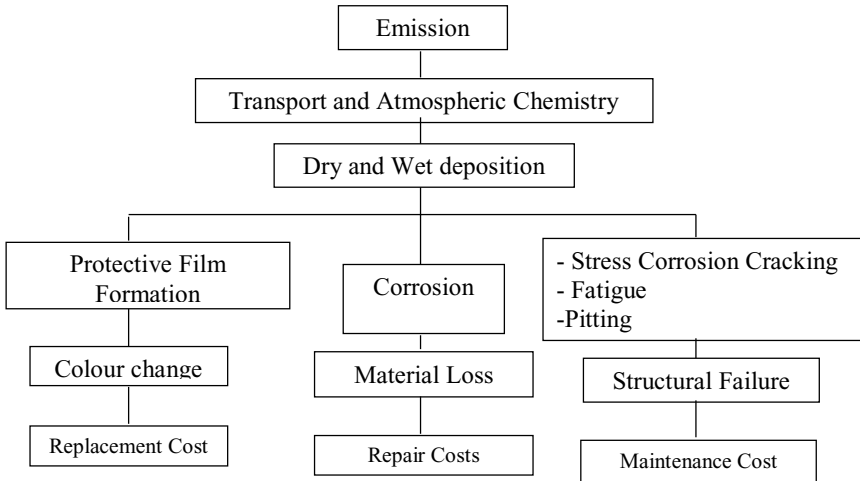


Figure 2.2 Impact pathways for effect of acidic deposition in metals (from EternE Project – 1998a).

2.8.0 FAILURE PROBABILITY OF CORRODED STRUCTURES

According to Melcher (1999), corrosion has many variables with uncertain nature. For this reason, the use of probabilistic model to describe the expected corrosion of structures is appropriate and desirable in reliability assessment.

The reliability of a structure is its ability to fulfil its design purpose for some specified time period. A fundamental assumption of structural design is that malfunction can occur in a finite number of failure modes described by a family of limit states. Hence, reliability is the probability that a structure will not attain each specified limit state during a specified reference period. The complementary event, i.e.

the probability that a structure will attain or exceed a specified limit state, is called the probability of failure.

The reliability (probability of survival or no failure) of a structure is defined as

$$P_s = 1 - P_f \dots\dots\dots 2.16$$

2.8.1 RELIABILITY AND FAILURE PROBABILITY

The limit state design process is defined by the principle of structural reliability, ISO 2394:1998 (E). Two types of limit states identified include Ultimate limit state and Serviceability limit state.

Total failure of a structure by any mechanism (fracture, buckling, overturning etc.) is considered to be failure under Ultimate limit state. Other forms of limit state may however cause a structure not to be fit for purpose. The function $g(\underline{x})$ describes the limit state as

- $g(\underline{x}) > 0$ limit state is satisfied (safe set)
- $g(\underline{x}) < 0$ failure occurs (unsafe set)
- $g(\underline{x}) \geq 0$ failure surface

with \underline{x} a vector of statistical variable which takes into account uncertainties.

$$\text{and } P_f = p(g(\underline{x}) < 0) = p(R - S < 0) \dots\dots\dots 2.17$$

From Melcher (2002) under normal distribution, the probability of failure P_f of a structure is calculated from

$$P_f = \Phi[-\mu_R - \mu_C] / \sqrt{(\sigma_R^2 + \sigma_S^2)} = \Phi[-\beta] \dots\dots\dots 2.18$$

Where μ_R and μ_C are means and

σ_R and σ_S are standard deviation of the load and resistance variables and ϕ is the cumulative density function of the standard normal distribution.

but reliability index (β) can be expressed as

$$\beta = -\phi^{-1}(P_f) \dots\dots\dots 2.19$$

In order to solve the probability of failure function of above, the Monte Carlo simulation or analytical methods (First Order Reliability Method) is employed.

2.8.2 CODE REQUIREMENT FOR RELIABILITY

As earlier noted, the product of failure probability and cost of failure defines the risk level or target level of reliability. According to Imran et al., (2004) uncertainties associated with modeling of deteriorating structures have strong influence on management decisions, such as when to inspect and scheduling of maintenance and repair actions. In this regard structural elements that are frequently inspected, show warning signs if failure is approaching or can redistribute its loads to other elements and hence less likely to cause loss of life at failure.

ISO 2394:1998 (E) suggested for serviceability limit state a target level of reliability, $\beta = 0$ for reversible and $\beta = 1.5$ for irreversible limit states

2.8.3 IMPACT OF LOCATION OF STRUCTURE AND CORROSION

Steel structures are not significantly affected by rural corrosion since high ozone level governs. However, urban and marine corrosions are significant since sulphate and chloride emission

prevails in both environments. Kayer (1989) noted that bearing and shear prevail in high levels of corrosion as their resistance is based on Webs (thin member) susceptible to thickness loss effect. In the same vein, compression members are more sensitive to corrosion since it is subject to buckling.

In the works of Park (1999), on the effects of time dependent loads and corrosion on bridge reliability, it was determined that failure due to shear force is a more immediate threat to a structure than due to moments.

Surveswaran et al (1998) examined the effect of corrosion penetration in I-girder structure reliability. The result indicates an adverse rate of corrosion for the bottom $\frac{1}{4}$ of the web and flange. Corrosion attack was noted for top and bottom surfaces of flanges as shown in figure 2.3 below

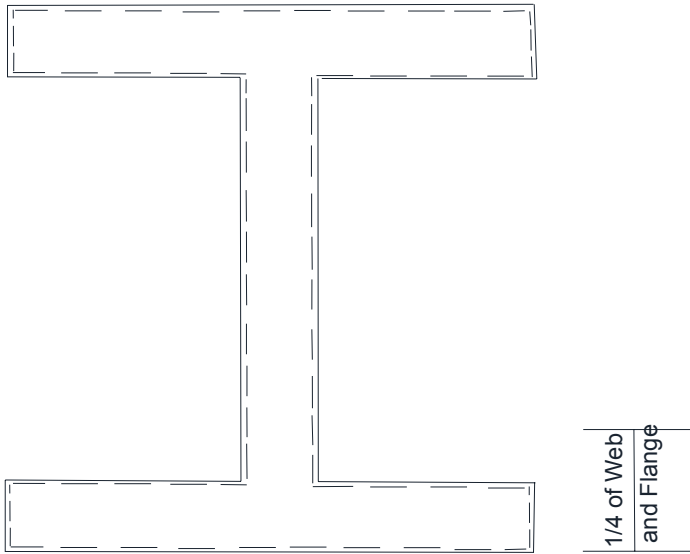


Figure 2.3 Show loss of material on a typical I-beam section

Lateral torsional buckling was determined as the most critical failure mode affecting corroded beam; followed by shear which affect the material loss of the bottom quarter of web and finally moment as compression flange is less significant.

BS EN 10025 clause 3/6.5.4 defines the maximum permitted thickness of steel parts which relates overall factor k and design minimum temperature, the chosen material yield strength and the Charpy test temperature of a chosen material grade. In this regard the maximum thickness is proportionally related to the value of k according to the code.

2.9.0 CHAPTER SUMMARY

The chapter reviewed the current efforts made to study the impact of human on climate and the effect of change in climate and air quality on man. It was observed from studies that the climate/weather will continue to change due to the damaging influence of man's activities on the earth.

Various building materials affected by climate change were identified with their impact. The impact of climate change was observed to be more noticeable in the urban areas than in the rural setting due to the effect of industrial gases and other anthropogenic effect in the atmosphere.

Further efforts will be made to look at the method of analysis of the climate change using the dose-response function approach while studying the impact of polluted environment on a bridge structure.

CHAPTER THREE

MATERIALS AND METHODS

3.1 METHODOLOGY

The impact of climate change on built infrastructure analysis would be achieved in two stages of examining the appropriate Dose-Response function for pollutants and evaluating their impact on a railway bridge structure.

In stage one, the mean and standard deviation of the pollutant data are obtained. From the mean, a dose-response value of the annual material loss is calculated for weathering steel. Evaluating the impact of climate parameters in the second stage involves probabilistic evaluation of the time to failure of various stages of corrosion on simply supported railway bridge structure using the moment and shear resistance and deflection checks.

3.2 DATA

The data for this work were obtained from the work of Brimblecombe et al (2008) on estimates of recession rate of limestone facades in London over a millennium.

This inhomogeneous data involve climate and pollutant parameters which have historic data, non-instrument and instrument data and future projections.

The record which represents climate around London region (Central England Temperature Record) can be extended to Guildford which has similar geographic and meteorologic characteristics. Key to the

merger of earlier historical records with instrument data as observed by Van Engelen et al (2001) was the high regression coefficient R^2 of 0.73 between the data.

Table 3.1 Climate and Pollution data used for the Dose-Response function (Data from Brimblecombe et al 2008)

Year	PM ₁₀	S ₀₂	N ₀₂	O ₃	HNO ₃	Temp.	pH	RH	Rain	CO ₂
	(µg)m ⁻³					(°C)		(%)	(mm)	ppm
1125	10	5	0.5	20	0.09	9.7	5.5	77	586	279
1175	13	5	0.5	20	0.09	9.8	5.5	77	611	279
1225	16	5	0.5	20	0.09	9.8	5.5	76	604	279
1275	19	5	0.5	20	0.09	9.8	5.5	76	609	279
1325	22	5	0.5	20	0.09	9.7	5.5	76	583	279
1375	14	6	0.5	20	0.09	9.9	5.5	77	577	279
1425	15	6	0.5	20	0.09	9.8	5.5	76	560	279
1475	15	6	0.5	20	0.09	9.8	5.5	76	558	279
1525	15	7	0.5	20	0.09	10	5.5	75	573	279
1575	26	20	4	20	0.24	9.9	5.5	76	549	275
1625	40	40	7	20	0.32	10	5.5	75	549	272
1675	60	120	20	15	0.47	9.8	5.5	75	605	272
1725	130	260	40	15	0.67	10.4	5.5	75	590	272
1775	140	280	40	15	0.67	10.2	5.5	74	609	277
1825	150	300	50	15	0.75	10.4	5.5	74	605	280
1850	160	320	50	15	0.75	10.4	5.5	74	591	280
1870	190	380	50	15	0.75	10.5	5.5	74	557	280

1890	200	400	58	15	0.81	10.4	5.5	74	624	285
1910	175	350	53	15	0.78	10.6	4.5	74	592	290
1930	160	320	53	15	0.79	10.9	4.5	74	579	295
1950	150	300	60	15	0.84	11.1	4	73	563	305
1970	70	150	75	40	1.52	10.9	4	73	591	321
1990	40	20	75	50	1.73	11.4	5	73	582	352
2010	30	17	40	40	1.15	11.8	5.2	72	590	383
2030	15	15	20	30	0.71	12.3	5.5	71	604	430
2050	14	14	20	30	0.73	12.9	5.5	71	574	530
2070	13	13	20	30	0.77	14.4	5.5	70	551	610
2090	12	12	20	30	0.73	13.4	5.5	68	584.2	730
Mean	68.36	120.75	27.13	22.1	0.57	10.7	5.2	74.1	423.49	330.36
Variance	4459	21073	628.5	79.3	0.19	1.43	0.20	4.69	20.58	12288.6
Standard										
Deviation	66.77	145.17	25.07	8.91	0.43	1.20	0.45	2.17	0.04	110.85
Coeff. Of										
Variation	0.98	1.20	0.92	0.40	0.76	0.11	0.08	0.03		

From table 3.1 above, temperature is seen to increase steadily from the reference year of 2010 with a low coefficient of variation of 0.11. Rainfall and relative humidity on the other hand has lowest coefficient of variation and a possible decline in the value from the reference year of 2010 moving to 2090. This is synonymous with the prediction of change in rainfall pattern for the environment and globally.

3.3 DESCRIPTION OF STUDY AREA

The study area is Guildford, a borough in the South East county of Surrey, United Kingdom and a total land area of 270.9km². According to Hutchinson (2006), Guildford was established around the year 500AD with its Norman Castle founded after 1066AD. It expanded with the arrival of a rail link between London and Portsmouth in 1845.

Guildford which is perched by the highlands of Surrey hills has River Wey, starting from the North Down of River Thames run through the town and serve as the main drainage channel to the sea and means of transportation. It is located within latitude 51° 13' – 51° 15'N and longitude 0° 33' – 0° 36'W or according to the ordinance survey plan between 147500 – 150500m.

The main soil type is the lower Greensand of the lower cretaceous, Mesozoic sedimentary formation.

From Wisley Guildford station Records (Wikipedia 2012) the annual temperature mean of Guildford is 10.3°C with a high of 14.55°C and a low of 6.1°C. Precipitation of the area has an annual average of 647.1mm. All the above data correlates with the Brimblecombe et al (2008) work for London area, hence their use in the present research.



Figure 3.1 Show map of study area Guildford according to Three Regions Climate Change group (2008)

3.4 THEORY OF ANALYSIS

The importance of the analysis is to determine the consistency and efficiency of a data set for their effective use in the estimation of the required dose-response function. The parameters determined in

this regard include the mean, standard deviation, variance and coefficient of variation.

3.4.1 MEAN OF POLLUTANTS AND CLIMATE PARAMETERS

The mean of each pollutant and climate parameter record is calculated using the following:

$$X = \frac{1}{N} \sum_{i=1}^N X_i \quad \dots \quad \dots \quad \dots \quad \dots \quad \dots \quad \dots \quad 3.1$$

Where X_i is the random variables of pollutants or climate parameter and N is the total number of observations.

3.4.2 Standard Deviation

This is a measure of variability. It indicates the dispersion or variation from the mean. Low value shows data points are close to mean where as high value point to a spread out from mean values.

$$\begin{aligned} \sigma_x &= \sqrt{\frac{1}{N} \sum_{i=1}^N (X_i - X)^2} \quad \dots \quad \dots \quad \dots \quad \dots \quad \dots \quad 3.2 \\ &= \sqrt{\frac{1}{N} \sum_{i=1}^N X_i^2 - \left(\frac{1}{N} \sum_{i=1}^N X_i\right)^2} \end{aligned}$$

3.4.3 VARIANCE (σ^2)

Variance measures the degree of spread out of a set of numbers.

$$\begin{aligned} \text{Var}(X) &= E[X^2] - X^2 \quad \dots \quad \dots \quad \dots \quad \dots \quad 3.3 \\ &= \sigma_x^2 \end{aligned}$$

3.4.4 COEFFICIENT OF VARIATION

This is defined as the ratio of the standard deviation σ_x to the mean X . It is a normalized measure of dispersion of a sample data which is expressed as a percent.

$$C_v = \sigma/X \quad \dots \quad \dots \quad \dots \quad \dots \quad 3.4$$

Where σ is the standard deviation of the set of numbers or variables and X is the mean.

3.5 EFFECT OF ANALYSIS ON MATERIALS

3.5.1 DOSE-RESPONSE FUNCTION AND ESTIMATION OF MATERIAL LOSS

In unsheltered condition, wet deposition (through rain) of SO_2 is the most important pollutant parameter for weathering steel and zinc. Several researchers have worked on the appropriate dose-response functions that will possibly capture the adverse effect of climate and pollutant parameters on built structures. These include the following:

Tidblad et al (2001), determined the dose-response function for weathering steel to be

$$\text{ML}(\mu\text{g}/\text{m}^2) = 34(\text{SO}_2)^{0.33} \exp[0.020\text{Rh} + f_{\text{ws}}(T)]t^{0.33} \dots \dots \dots 3.5$$

Where $f_{\text{ws}}(T) = 0.059(T-10)$ when $T \leq 10^\circ\text{C}$ and $f_{\text{ws}}(T) = -0.036(T-10)$ otherwise.

Based on regression coefficient $R^2 = 0.68$ for explained variability.

In this regard the UN/ECE 8-year programme, Dose Response Function as in Mikhailov (2001) for unsheltered condition is appropriate to work with, that is,

$$\ln(\text{ML}) = 3.54 + 0.33 \ln(t) + 0.13 \ln(\text{SO}_2) + 0.020\text{RH} + 0.059(T-10)$$

for $T \leq 10^\circ\text{C}$ 3.9

and

$$\ln(\text{ML}) = 3.54 + 0.33 \ln(t) + 0.13 \ln(\text{SO}_2) + 0.020\text{RH} - 0.036(T-10)$$

for $T > 10^\circ\text{C}$ 3.10

Other functions considered for this work include,

The result of the Meta-analysis by Lipfert (1987) with critical and site results indicated for unsheltered annual loss for zinc as:

$$\text{ML} = [t^{0.78} + 0.46 \log_e(\text{H}^+)]. [4.24 + 0.55 \cdot f_2 \cdot \text{SO}_2 + 0.029\text{CL} + 0.029\text{H}^+]$$

..... 3.11

Where f_2 is a function of time and relative humidity exceeds 85%

Butlin et al (1992a) suggested for the Natural Materials Exposure programme for unsheltered zinc in one year loss as:

$$\text{ER} = 1.38 + 0.38\text{SO}_2 + 0.48\text{P} \dots \dots \dots 3.12$$

However, this function has been modified by Kucera (1994) to include the effect of ozone and time of wetness as in

$$\text{ML} = 14.5 + 0.043\text{Tow} \cdot \text{SO}_2 \cdot \text{O}_3 + 0.08\text{H}^+ \dots \dots \dots 3.13$$

Dose-Response function for the calculation of a year corrosion loss for carbon steel based on BS EN ISO 9223:2012 is

$$r_{\text{corr}} = 1.77 \cdot [\text{SO}_2]^{0.52} \cdot \exp^{(0.020\text{RH} + \text{fst})} + 0.102[\text{CL}]^{0.62} \exp^{(0.033\text{RH} + 0.040\text{T})} \dots \dots \dots 3.14$$

where $f_{st} = 0.150 (T-10)$ when $T \leq 10^{\circ}\text{C}$, otherwise $- 0.054 (T-10)$,
 r_{corr} = first year corrosion rate of carbon steel in $\mu\text{m}/\text{year}$ and other terms as defined in the appendix.

All the Dose-Response functions above are used to determine the thickness loss from the surface of a corroded steel structure, depending on the parameter of interest.

3.5.2 BS EN ISO 9223:2012

ISO 9223 is the code for the classification, determination and estimation of corrosion of metals. Based on comparative estimation of the various dose-response function thickness losses, the function for this code was chosen for the analysis.

This is because it gives the result close to the average thickness loss calculated in this work from other functions. The second reason for the choice of the dose-response function for the analysis is because of the critical influence of the parameters in the corrosion rate of metals.

3.5.2.1 CLASSIFICATION

The classification defines the corrosivity of the environment by categories.

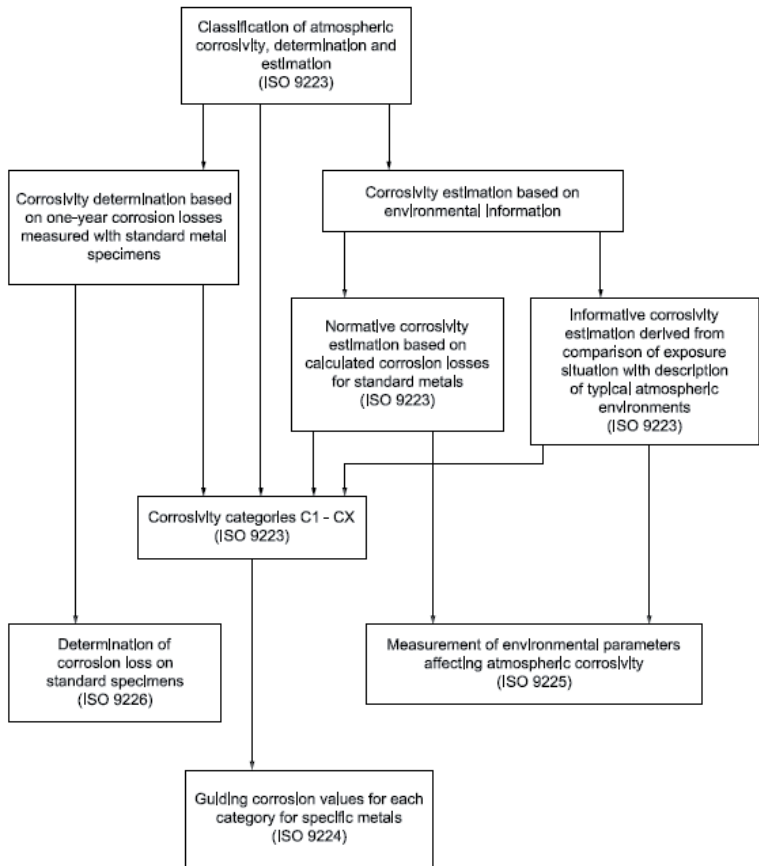


Figure 3.2 Classification of atmospheric corrosivity according to ISO 9223

Categorization is based on the one year corrosion rate experiment on standard specimens. The principal elements in the corrosion of metals are temperature, humidity, pollution by sulphur and the acidity of the air.

Table 3.2: Categories of corrosivity of the atmosphere according to ISO 9223

Category	Corrosivity
C1	Very low
C2	Low
C3	Medium
C4	High
C5	Very high
CX	Extreme

The categories, their nature of corrosivity and prevailing environment conditions are explained below.

	Corrosivity	Typical environments — Examples	
		Indoor	Outdoor
C1	Very low	Heated spaces with low relative humidity and insignificant pollution, e.g. offices, schools, museums	Dry or cold zone, atmospheric environment with very low pollution and time of wetness, e.g. certain deserts, Central Arctic/Antarctica
C2	Low	Unheated spaces with varying temperature and relative humidity. Low frequency of condensation and low pollution, e.g. storage, sport halls	Temperate zone, atmospheric environment with low pollution ($\text{SO}_2 < 5 \mu\text{g}/\text{m}^3$), e.g. rural areas, small towns Dry or cold zone, atmospheric environment with short time of wetness, e.g. deserts, subarctic areas

C3	Medium	Spaces with moderate frequency of condensation and moderate pollution from production process, e.g. food-processing plants, laundries, breweries, dairies	Temperate zone, atmospheric environment with medium pollution (SO ₂ : 5 µg/m ³ to 30 µg/m ³) or some effect of chlorides, e.g. urban areas, coastal areas with low deposition of chlorides Subtropical and tropical zone, atmosphere with low pollution
C4	High	Spaces with high frequency of condensation and high pollution from production process, e.g. industrial processing plants, swimming pools	Temperate zone, atmospheric environment with high pollution (SO ₂ : 30 µg/m ³ to 90 µg/m ³) or substantial effect of chlorides, e.g. polluted urban areas, industrial areas, coastal areas without spray of salt water or, exposure to strong effect of de-icing salts Subtropical and tropical zone, atmosphere with medium pollution
C5	Very high	Spaces with very high frequency of condensation and/or with high pollution from production process, e.g. mines, caverns for industrial purposes, unventilated sheds in subtropical and tropical zones	Temperate and subtropical zone, atmospheric environment with very high pollution (SO ₂ : 90 µg/m ³ to 250 µg/m ³) and/or significant effect of chlorides, e.g. industrial areas, coastal areas, sheltered positions on coastline

CX	Extreme	Spaces with almost permanent condensation or extensive periods of exposure to extreme humidity effects and/or with high pollution from production process, e.g. unventilated sheds in humid tropical zones with penetration of outdoor pollution including airborne chlorides and corrosion-stimulating particulate matter	Subtropical and tropical zone (very high time of wetness), atmospheric environment with very high SO ₂ pollution (higher than 250 µg/m ³) including accompanying and production factors and/or strong effect of chlorides, e.g. extreme industrial areas, coastal and offshore areas, occasional contact with salt spray
----	---------	--	---

3.5.2.2 DETERMINATION OF CORROSION RATE

Determination of the corrosion rate is based on one year exposure of metals and the measurement of the corrosion of the standard specimens according to ISO 9224. From this test, the numerical values of the first year corrosion rate of different metals under various corrosivity categories were estimated as below.

Table 3.3 Corrosion rate for first year exposure under various corrosivity categories from ISO 9223

Corrosivity category	Corrosion rates of metals				
	Unit	Carbon steel	Zinc	Copper	Aluminium
C1	g/(m ² .a)	$r_{\text{corr}} \leq 10$	$r_{\text{corr}} \leq$	$r_{\text{corr}} \leq 0,9$	Negligible
	µm/a	$r_{\text{corr}} \leq 1,3$	0,7 $r_{\text{corr}} \leq$	$r_{\text{corr}} \leq 0,1$	

			0,1		
C2	g/(m ² .a) µm/a	10 < r _{corr} ≤ 200 1,3 < r _{corr} ≤ 25	0,7 < r _{corr} ≤ 5 0,1 < r _{corr} ≤ 0,7	0,9 < r _{corr} ≤ 5 0,1 < r _{corr} ≤ 0,6	r _{corr} ≤ 0,6 —
C3	g/(m ² .a) µm/a	200 < r _{corr} ≤ 400 25 < r _{corr} ≤ 50	5 < r _{corr} ≤ 15 0,7 < r _{corr} ≤ 2,1	5 < r _{corr} ≤ 12 0,6 < r _{corr} ≤ 1,3	0,6 < r _{corr} ≤ 2 —
C4	g/(m ² .a) µm/a	400 < r _{corr} ≤ 650 50 < r _{corr} ≤ 80	15 < r _{corr} ≤ 30 2,1 < r _{corr} ≤ 4,2	12 < r _{corr} ≤ 25 1,3 < r _{corr} ≤ 2,8	2 < r _{corr} ≤ 5 —
C5	g/(m ² .a) µm/a	650 < r _{corr} ≤ 1500 80 < r _{corr} ≤ 200	30 < r _{corr} ≤ 60 4,2 < r _{corr} ≤ 8,4	25 < r _{corr} ≤ 50 2,8 < r _{corr} ≤ 5,6	5 < r _{corr} ≤ 10 —
CX	g/(m ² .a) µm/a	1500 < r _{corr} ≤ 5500 200 < r _{corr}	60 < r _{corr} ≤ 180	50 < r _{corr} ≤ 90 5,6 < r _{corr}	r _{corr} > 10 —

G_k , the characteristic value of permanent action

Q_k , the characteristic value of variable action

P , the characteristic value of a prestressing force where applicable

ψ_0 , is the combination factor for variable action

3.6.1.2 CALCULATION OF MOMENT AND SHEAR RESISTANCE

These are obtained using the elastic method for simply supported structure as

Moment, $M = wL^2/8$ and the moment of resistance for the main girder is calculated using $M_D = M_R/\gamma_m\gamma_{f3}$ according to clause 9.9.1.2 of BS 5400 part 3

and

Shear Force, $V = wL/2$ while the shear resistance is given as

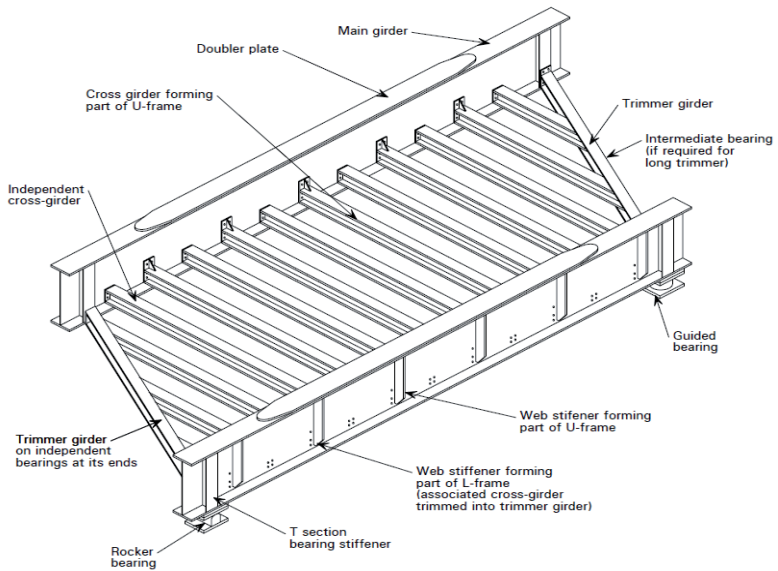
$V_D = [t_w (d_w - h_h) / \gamma_m\gamma_{f3}]T_1$ clause 9.9.2.2 BS 5400 part 3

Where w is the load in kN/m and L is the span length, M_D is the bending resistance, M_R is the limiting moment of resistance, γ_m is the safety factor and γ_{f3} is partial factor on characteristic yield stress.

For the shear resistance V_D is the shear resistance of the web panel, t_w the thickness of the web, d_w is the overall depth of the girder, h_h height of any opening, γ_m and γ_{f3} as defined above and T_1 is the limiting shear strength of the web panel.

3.6.1.3 VERIFICATION OF SERVICEABILITY LIMIT STATE OF DEFLECTION

The check is made to verify the damage that will likely adversely affect the durability of the structure. Bridges structures are



Longitudinal section on deck

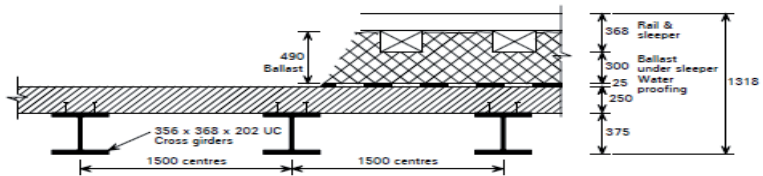


Fig 3.3 Half Through bridge structure and components (SCI Publication P318)

3.7 CHAPTER SUMMARY

The method of analysis was considered in this section. Two stages were involved, first is the determination of the rate of material loss through the appropriate dose-response function and the second stage is the use of the calculated thickness loss to determine the bending resistance, shear resistance and deflection of the single span railway bridge.

4.1

STAGE ONE ANALYSIS:

CLIMATE AND CLIMATE CHANGE

CHAPTER FOUR

RESULTS AND DISCUSSIONS

The section describes the results achieved and the method used in the implementation. Discussion of the results involved detailing the effect of the result of climate change on built structure such as a Railway Bridge located in Guilford, Surrey.

4.1 CLIMATE CHANGE PREDICTIONS

Climate change according to IPCC Climate Change 2007: Synthesis Report refers to observable change through statistical analysis of means and other variable properties over a period of time usually above a decade. This change in climate with time may be due to natural causes or it may be due to human activity.

Warming of the climate system it has been argued is responsible for the increase in global average temperature, melting of ice and rise in global average sea level. As observed by Houghton (2004), various human activities in the industry, in the field, in form of deforestation, in transportation or at home are resulting in emissions of gaseous pollutants of increasing amounts. Carbon dioxide it is observed is a good absorber of radiated heat coming from the earth's surface, increases in the quantity of carbon dioxide acts like a shield covering over the earth surface, thereby causing the earth to warm more than it would normally be.

4.1.1 EMISSION SCENARIOS

Climate models predict future climate change due to human activities. A good future climate projection depends on equally good assumption on human behaviour and activities which include population growth, economic growth, energy use and the sources of energy generation. IPCC Special Report on Emissions Scenarios (SRES, 2000) describes the group of four scenario families A1, A2, B1 and B2 used in developing the projections of future climate.

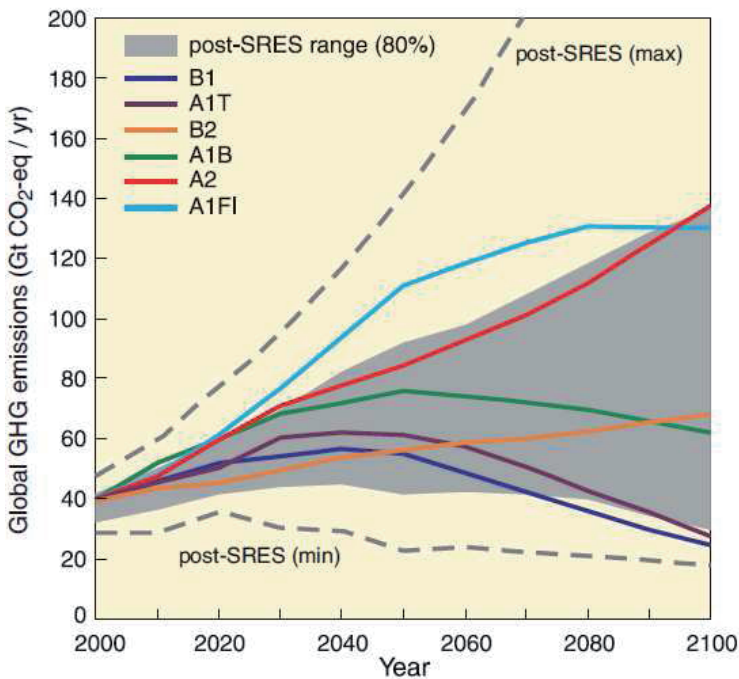


Figure 4.1 Scenarios for GHG emissions from 2000 to 2100 according to SRES, 2000

The SRES Scenarios storylines as explained by Houghton (2004) is as follows:

A1: Describes a world with rapid economic growth, a global population with peak in mid-century and declines thereafter, and a new and technology driven future. Three further groups within A1 according to technology include: fossil fuel intensive A1F1, non-fossil fuel energy source (A1T) and a balance across all source (A1B).

A2: Scenario storyline defines a heterogeneous world with main theme of self-reliance and preservation of local identities. This scenario presents a slower growth than previous case but with some economic development and technological changes envisaged.

B1: In this case, the world is shown to converge with same population growth peak at mid-century. However economic growth will be towards a service and information industry with emphasis on global solution to economic, social and environmental sustainability.

B2: Emphasis local solutions to economic, social and environmental sustainability. Nonetheless, global population is projected to increase at a lower rate than A2, slower level of economic development and diverse technological changes than in B1 and A1.

Table 4.1 show projected global average surface warming and sea level rise at the end of 21st century according to Climate Change 2007: Synthesis Report

Case	Temperature change (°C at 2090 – 2099 relative to 1980 - 1999)		Sea level rise (m at 2090 – 2099 relative to 1980 - 1999)
	Best estimate	Likely range	Model-based range excluding future rapid dynamical changes in ice flow
Constant year 2000 concentration	0.6	0.3 – 0.9	Not available
B1 Scenario	1.8	1.1 – 2.9	0.18 – 0.38
A1T Scenario	2.4	1.4 – 3.8	0.20 – 0.45
B2 Scenario	2.4	1.4 – 3.8	0.20 – 0.43
A1B Scenario	2.8	1.7 – 4.4	0.21 – 0.48
A2 Scenario	3.4	2.0 – 5.4	0.23 – 0.51
A1F1 Scenario	4.0	2.4 – 6.4	0.26 – 0.59

Models such as those of HadCM3 considered these factors in obtaining the input parameters used in the determination of their effect on climate change.

Uncertainties still exist due to the probabilistic nature of the emission scenarios earlier pointed out. However, the emission uncertainties are being tackled by the UKCP09 through three scenarios which are labelled High (IPCC SRES: A1F1), Medium (IPCC SRES: A1B) and Low (IPCC SRES: B1) according to Nakicenovic et al., (2000).

4.1.2 AIR POLLUTION AND CLIMATE

According to Hulme et al (2002) in Brimblecombe et al (2008), “London climate will change over the current century. From the model analysis using the HadCM3, temperature is expected to rise by 4°C by 2080 under the A2 Emission Scenario and precipitation will increase in winter and decrease in the summer”. London air

pollution was observed to have increased from the industrial revolution period (1700 -1970), see table 4.2 below and the analysis in appendix. The decrease in the volume of SO₂ and other pollutants after the 1970's is indicative of the effect of regulation and monitoring that followed. First the use of coal for domestic and industrial purposes was minimized, then regulation on smoke abatement was developed and following the era of European Union, monitoring activities were improved.

Table 4.2 Mean values of parameters from differing time periods.

Year	PM ₁₀	SO ₂	NO ₂	O ₃	HNO ₃	Temp.	pH	RH	Rain	CO ₂
	(µg)m ⁻³					(°C)		(%)	(mm)	ppm
1125-1675	22.08	19.17	2.96	19.58	0.15	9.83	5.50	76.00	580.33	280.21
1675-1970	144.09	289.09	49.91	17.27	0.80	10.51	5.05	74.00	591.73	287.00
1970-2010	46.67	62.33	63.33	43.33	1.47	11.37	4.73	72.67	578.67	352.00
2010-2090	16.80	14.20	24.00	32.00	0.82	12.96	5.44	70.40	580.20	536.60

4.2 TEMPERATURE

Temperature projection is one of the widely used parameter in the determination of global climate change. Houghton (2004) describes a global average rise due to increase in greenhouse gases of 0.6°C by 2000 and projected to increase in the range of 2°C to 6°C in 2100.

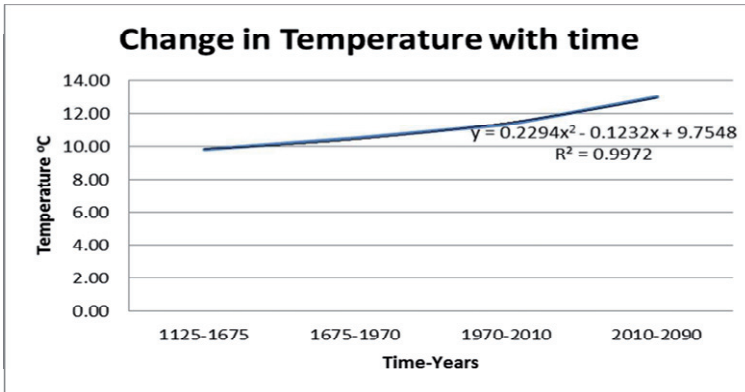


Figure 4.2 show Temperature change with time as a result of increase in greenhouse gases.

During the 20th century, the annual mean of Central England temperature warmed by about 1.1° C. The 1990s were exceptionally warm, by historical standards, about 0.6° C warmer than the 1961-1990 average as observed in the Hadley Centre (Met office) records.

Temperature of South England is project to increase the highest in summer under the high emission scenario according to Land Use Consultants (2003) and by 2080s the increase is expected to reach 5°C. For low emission scenario, the summer temperature is

expected to rise between 2 - 3°C for the same period. The impact of this will be a rise in the number of extreme warm days with a corresponding decrease in the number of heating degree days especially in winter.

4.3 RELATIVE HUMIDITY

There will be change in rainfall patterns, making summer drier and winter wetter, with the resultant decrease in relative humidity. It is projected that rainfall and evaporation will decrease in summer and autumn under the high and low emission scenarios. The reduction in relative humidity is shown in the figure 4.3 below to be slow with time.

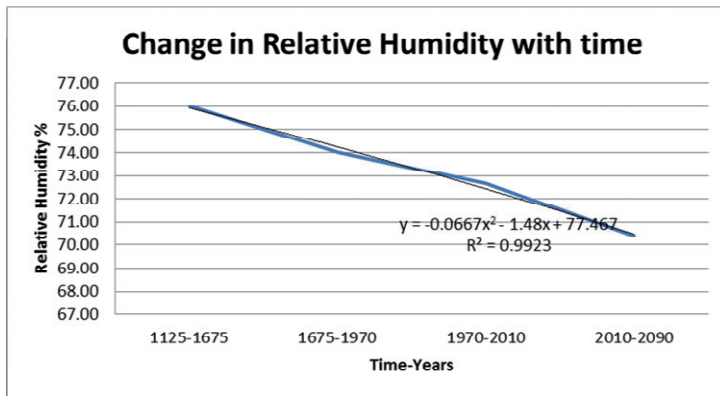


Figure 4.3 Reduction in Relative humidity with time

4.4 SULPHUR DIOXIDE

The dominate form of emission in United Kingdom is burning of fuels containing sulphur, typical of coal and heavy oils, used by power plants and refineries. Domestic use of coals for heating and

other purposes is reducing in significance, though still in use in some regions in the country. Pollution caused by SO₂ emission cause acidification of soils and water, often further down the source of production in form of acid rain.

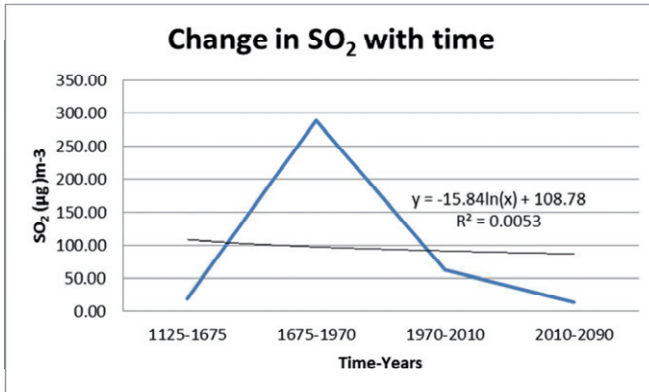


Figure 4.4 Sulphur dioxide reductions with Time

From the graph Fig 4.4 above, it is evident that the policy on pollution abatement embarked upon since the 1970's has given rise to a reduction in sulphate concentration in the United Kingdom.

4.5 CARBON DIOXIDE

It is projected, according to UKCIP98, that by the 2020s, carbon dioxide concentrations for the Medium-low and Medium-high scenarios would be, respectively, 19% and 34% higher than the 1961-90 average of 334ppm, and by the 2080s, 49% and 109% higher. As shown in in table 4.2 and figure 4.5 below, emission from carbon dioxide is increasing rapidly and becoming larger with time.

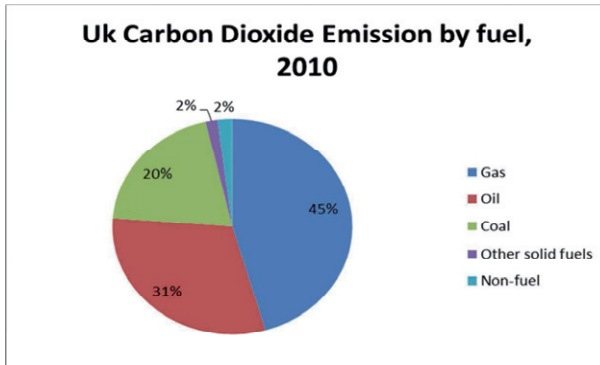


Figure 4.5 show an extract of the carbon dioxide emission by fuel sources in 2010 (DECC, 2012)

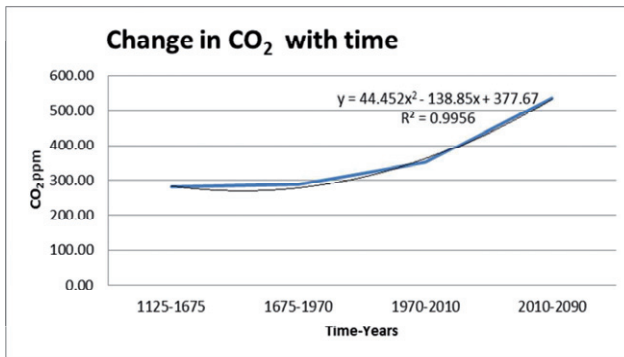


Figure 4.6 show the projected increase in carbon dioxide Concentration with time

4.6 AIR QUALITY ANALYSIS – SO₂, NO₂, O₃, CO₂

4.6.1 ESTIMATION OF DOSE-RESPONSE FUNCTIONS

Table 4.3 below shows the comparison of the result of eight dose-response functions from various authors and the result obtained from each. The different results obtained may be attributed

to the nature of analysis and the parameters input used in the analysis. For example, while some used SO₂, RH and Temperature only in their formulation others added the effect of O₃, PH and particulate matter in the equation.

An average dose-response function was determined as in table 4.4 and figure 4.7 and used in the calculation of the thickness loss in the work. The average function is a plot of the mean of the highest and lowest at all the points of the one year functions.

Table 4.4 Mass Loss based on several dose-response functions and an average dose-response function.

Time(t)	Year	PM10	S02	N02	O3	HN03	Temp.	pH	RH	Rain	Avg. Dose-Response
Years		$(\mu\text{g})\text{m}^{-3}$					$(^{\circ}\text{C})$		$(\%)$	(mm)	(μm)
1	2010	30	17	40	40	1.15	11.8	5.2	72	582	26.54
20	2030	15	15	20	30	0.71	12.3	5.5	71	590	68.75
40	2050	14	14	20	30	0.73	12.9	5.5	71	604	94.44
60	2070	13	13	20	30	0.77	14.4	5.5	70	574	112.93
80	2090	12	12	20	30	0.73	13.4	5.5	68	551	126.41

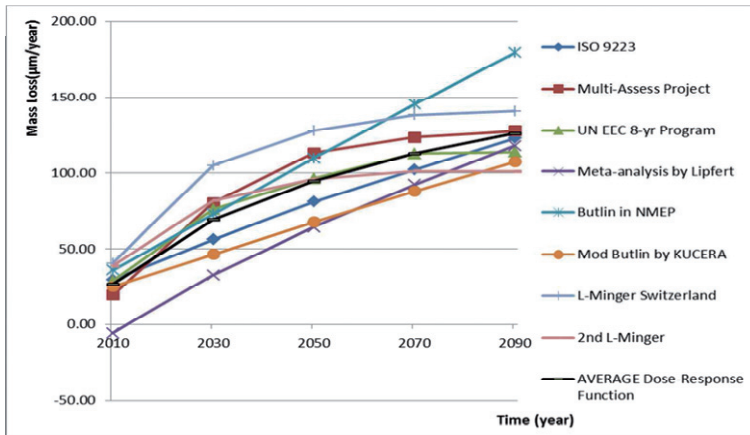


Figure 4.7 show the comparison of the dose-response functions from various researchers and the average dose-response function

DISCUSSION OF RESULTS

The following regression functions were based on the curves generated from excel for the various authors:

ISO 9223 function, $y = 2390.9\ln(x) - 18154$ with coefficient $R^2 = 0.9978$ 4.1

The parameters for this function include sulphur dioxide, temperature, relative humidity and chloride. Since the structure is outside the coastal area the chloride factor was ignored.

Multi-Assess Project function, $y = 2675.1\ln(x) - 20306$ with error coefficient, $R^2 = 0.8353$ 4.2

Multi-assess project according to Kucera (2005) considered such factors as sulphate dioxide, relative humidity, precipitation, acid concentration in rain, time in years and particulate matter in the dose-response function.

UN ECE 8-yr Programme function, $y = 2131.3\ln(x) - 16167$ the coefficient, $R^2 = 0.8659$ 4.3

Using the Mikhailov (2001) function, the parameters in use include time in years for the data, sulphur dioxide, relative humidity and temperature.

Meta-Analysis by Lipfert (1987) gave regression function, $y = 3147.9\ln(x) - 23944$ with $R^2 = 0.9947$ 4.4

Parameters used for the calculation include time in years for the data, acid concentration in rain, a function which defines the fraction of time relative humidity exceeds 85%, sulphur dioxide, and chloride concentration.

Butlin in NMEP function, $y = 3683.7\ln(x) - 27982$ and coefficient $R^2 = 0.9999$ 4.5

Material loss by Butlin (1992) used such factors as sulphur dioxide, and precipitation in its estimation.

Mod. Butlin by Kucera (1994) function, $y = 2112.5\ln(x) - 16042$ the coefficient $R^2 = 0.9999$ 4.6

A modification made by Kucera (1994), added the ozone concentration, time of wetness and acid concentration in rain as factors in the calculation of the dose-response function which gave the above regression function.

L-Minger in Switzerland (2002) function, $y = 2401.6\ln(x) - 18203$ with coefficient $R^2 = 0.7944$ 4.7

In this analysis, such parameters as sulphur dioxide, time of wetness, time in years and ozone were considered.

2nd L-Minger without Ozone (2002) function, $y = 1482.7\ln(x) - 11222$ the coefficient $R^2 = 0.7513$ 4.8

A less accurate prediction was obtained disregarding the ozone factor to obtain the above function.

Ave. Dose-Response with regression function, $y = 2503.2\ln(x) - 19002$ and error coefficient, $R^2 = 0.9525$ 4.9

From the outputs of the various functions, it is observed that the function closest to the average value is the ISO 9223 function hence the use in the work for the calculation of the thickness loss.

Table 4.5: Annual max/min corrosion rate with the average corrosion based on the all the dose-response functions.

Time(t)	Year	Min	Max	Average
Years		(μm)	(μm)	(μm)
1	2010	-5.62	40.58	17.48
20	2030	32.66	104.91	68.79
40	2050	64.12	128.02	96.07
60	2070	87.68	145.24	116.46
80	2090	101	179.29	140.15

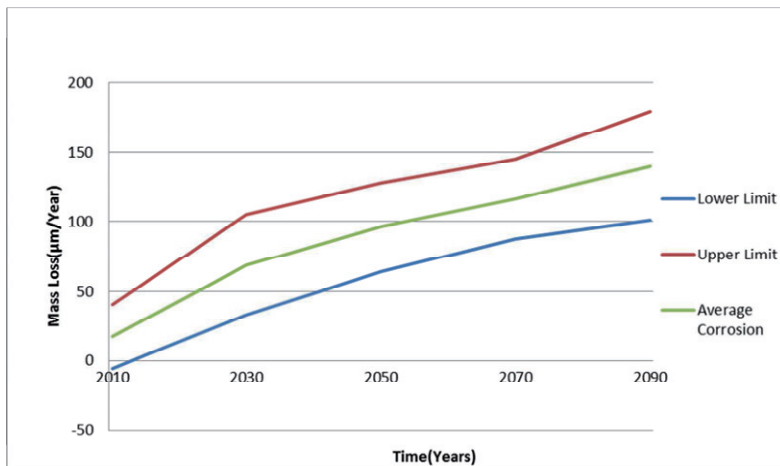


Figure 4.8 Average corrosion rate against time

DISCUSSION

Figure 4.8 shows the average corrosion rate over time, which describes the average of the upper and lower bounds of the various dose-response functions stated above. It is obtained as shown in table 4.5 above by establishing the highest and lowest points in

figure 4.7 for comparison of the dose-response function from various researchers. The maximum and minimum points obtained is averaged to establish the average corrosion rate against time. A plot of the maximum, minimum and the average values is shown in figure 4.8 which compares with the ISO 9223 result for the same time frame.

4.6.2 ANALYSIS OF THE POLLUTANTS

According to ISO 9223 categorization, the table 4.6 shows the values of the thickness loss with their classification while table 4.7 indicates the calculation of the thickness losses against time in years and the parameters used.

Table 4.6- classification of mass loss according to ISO standard

Year	ISO 9223	ISO Classification	
	(μm)	Range	Category
2010	29.58	25<ML<50	C3
2030	56.02	50<ML<80	C4
2050	80.72	80<ML<200	C5
2070	102.20	80<ML<200	C5
2090	123.09	80<ML<200	C5

Table 4.7 Calculation of thickness loss against time

Time	Year	PM ₁₀	S _O ₂	NO ₂	O ₃	HNO ₃	Temp.	pH	RH	Rain	ISO 9223
Year		(µg)m ⁻³					(°C)		(%)	(mm)	(µm)
1	2010	30	17	40	40	1.15	11.8	5.2	72	582	29.58
20	2030	15	15	20	30	0.71	12.3	5.5	71	590	56.02
40	2050	14	14	20	30	0.73	12.9	5.5	71	604	80.72
60	2070	13	13	20		0.77	14.4	5.5	70	574	102.2
					30						
80	2090	12	12	20	30	0.73	13.4	5.5	68	551	123.09
	Mean	16.8	14.2	24	32	0.82	12.96	5.44	70.4	580	
	Variance	44.56	2.96	64	16	0.03	0.81	0.01	1.84	311	
	Standard Dev.	6.68	1.72	8	4	0.17	0.9	0.12	1.36	17.7	
	Coeff. Of Var.	0.4	0.12	0.33	0.13	0.2	0.07	0.02	0.02	0.03	
	STD yr 2010-Mean	13.2	2.8	16	8	0.33	-1.16	0.24	1.6	1.8	

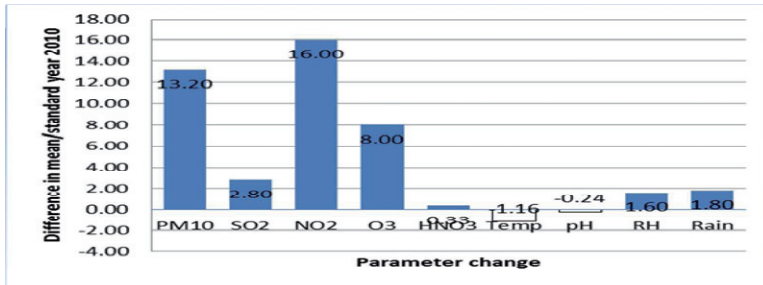


Figure 4.9 Difference in mean against various pollutant parameter change

4.6.2.1 TIME VARIATION OF PARAMETERS

Each of the parameters is analyzed for the effect of change in value on thickness loss. A change in percentage made an increase in the value of each of the parameters. This indicates that with an increase each year of the parameters the thickness loss tends to increase

Table 4.8 - Effect of Percentage change on parameters relative to 2050 values

%age change	2050 Reference year parameters						ISO 9223 (μm)	ISO 9223 DRF1(μm)
	S _O ₂ (μg)m- 3	Thicknes s Loss (μm)	Temp (°C)	Thickness Loss (μm)	RH (%)	Thicknes s Loss (μm)		
-20	11.2	21.99	10.32	28.39	56.8	18.59	29.58	29.58
-10	12.6	23.38	11.61	26.48	63.9	21.43	26.44	56.02
0	14	24.70	12.9	24.70	71	24.70	24.70	80.72
10	15.4	25.95	14.19	23.04	78.1	28.47	21.48	102.20
20	16.8	27.15	15.48	21.49	85.2	32.81	20.90	123.10

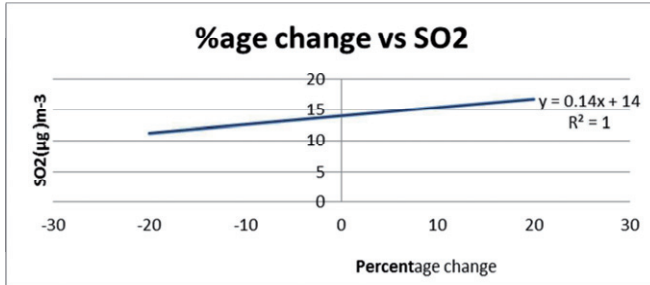


Figure 4.10 show increase in SO₂ with percentage increase

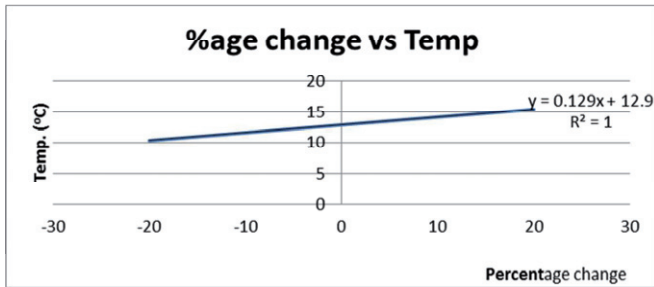


Figure 4.11 show increase in temperature with percentage increase

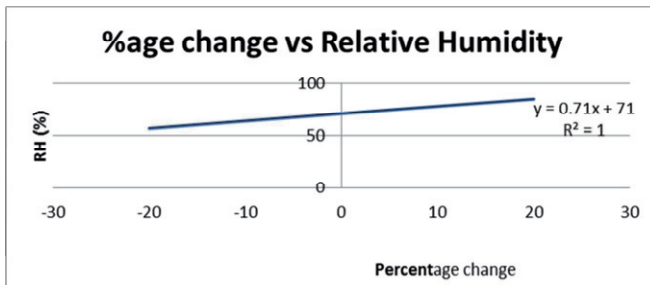


Figure 4.12 show increase in relative humidity with percentage increase

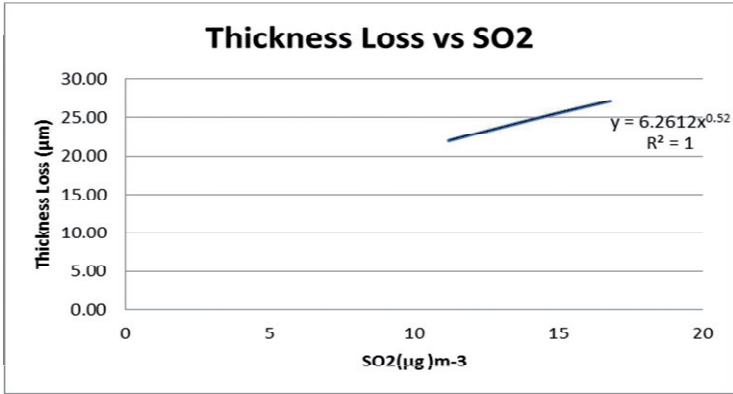


Figure 4.13 Increase in thickness loss with SO₂ increase

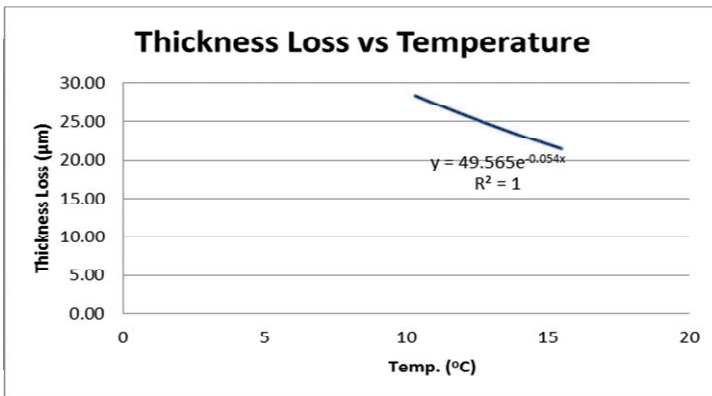


Figure 4.14 show a decrease in thickness loss with increase in temperature

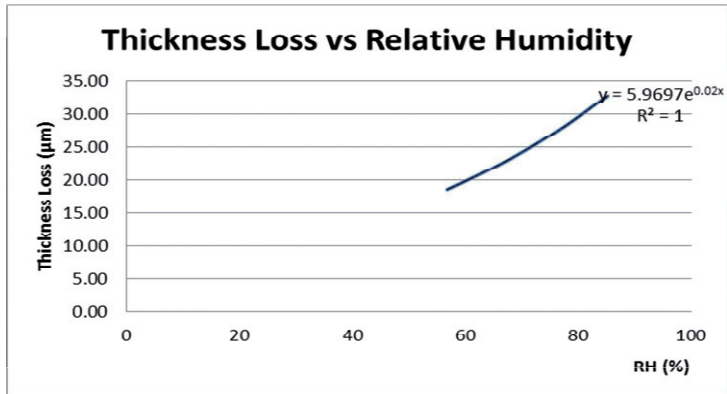


Figure 4.15 show increase in thickness loss due to increase in relative humidity

DISCUSSION

From the figures above, increase in temperature does not increase thickness loss as shown in figure 4.14 as against other parameters sulphur dioxide and relative humidity which increases thickness loss with their increase. Example, from the figures, a 10% increase in SO_2 will cause a 5% increase in thickness loss, which for a 20mm thick web will give rise to a reduction of 1mm thickness. A 10% increase in temperature on the other hand will cause 7% decrease in thickness loss. Increase in relative humidity by 10% will cause a 15% increase in thickness loss. It is therefore observed that increase in relative humidity will increase the amount of water vapour hence dissolved SO_2 and other gases and also increase in the time of wetness of corrosive materials on the structure.

4.6.2.2 SPATIAL VARIATION OF PARAMETER

In this regard, it is observed that location affects the rate of loss of materials from steel exposed to the climate change. Materials exposed to the rural area is least affected while those in industrial environment is most affected as seen in figures below. Table 4.9 - 4.11 shows the use of the ISO 9223 dose-response function to obtain the thickness losses over time for rural, urban and industrial environments. To obtain these values, the SO₂ is varied for the rural, urban and industrial areas while the temperature and relative humidity is kept constant. A plot of the thickness loss against time for various environments gives the rate of corrosion.

Table 4.9 : Rural values of SO₂(2 < SO₂<15)

Time	Year	PM ₁₀	SO ₂	NO ₂	O ₃	HNO ₃	Temp.	pH	RH	Rain	ISO 9223
Year		(µg)m ⁻³					(°C)		(%)	(mm)	(µm)

1	2010	30	17	40	40	1.15	11.8	5.2	72	582	29.58
20	2030	15	15	20	30	0.71	12.3	5.5	71	590	56.02
40	2050	14	14	20	30	0.73	12.9	5.5	71	604	80.72
60	2070	13	13	20	30	0.77	14.4	5.5	70	574	102.20
80	2090	12	12	20	30	0.73	13.4	5.5	68	551	123.09

Table 4.10 : Urban values of
SO₂(5<SO₂<100)

Time	Year	PM ₁₀	SO ₂	NO ₂	O ₃	HN0 ₃	Temp.	pH	RH	Rain	ISO 9223	ISO 9223
Year		(µg)m ⁻³					(°C)		(%)	(mm)	(µm)	(µm)
1	2010	30	78	40	40	1.15	11.8	5.2	72	582	65.32	65.32
20	2030	15	69	20	30	0.71	12.3	5.5	71	590	58.47	123.79
40	2050	14	64	20	30	0.73	12.9	5.5	71	604	54.43	178.22
60	2070	13	60	20	30	0.77	14.4	5.5	70	574	47.58	225.80
80	2090	12	55	20	30	0.73	13.4	5.5	68	551	46.12	271.92

Table 4.11 : Industrial values of SO₂(50< SO₂ <400)

Time	Year	PM ₁₀	SO ₂	NO ₂	O ₃	HN0 ₃	Temp.	pH	RH	Rain	ISO 9223	ISO 9223
Year		(µg)m ⁻³					(°C)		(%)	(mm)	(µm)	(µm)
1	2010	30	360	40	40	1.15	11.8	5.2	72	582	144.68	144.68
20	2030	15	315	20	30	0.71	12.3	5.5	71	590	128.78	273.47
40	2050	14	295	20	30	0.73	12.9	5.5	71	604	120.49	393.96
60	2070	13	270	20	30	0.77	14.4	5.5	70	574	104.02	497.98
80	2090	12	250	20	30	0.73	13.4	5.5	68	551	101.35	599.32

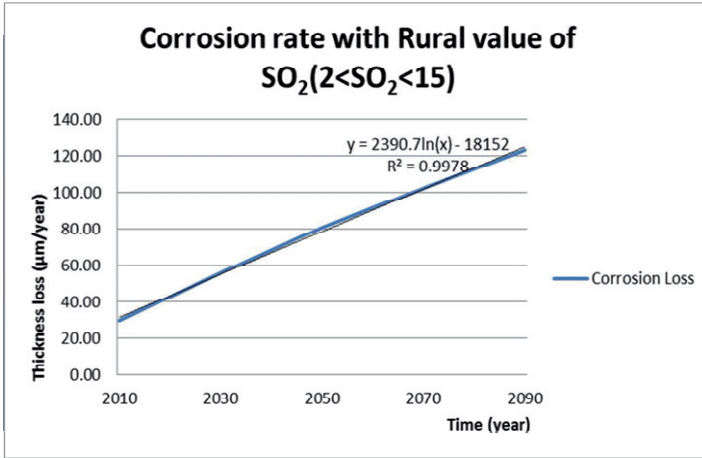


Figure 4.16 Corrosion rate for rural environment

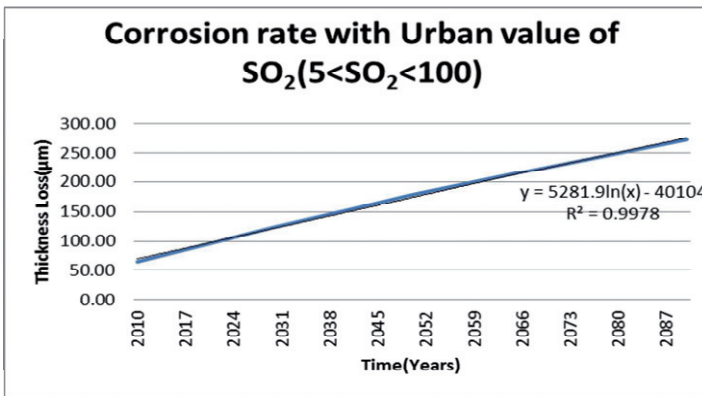


Figure 4.17 Corrosion rate for urban environment

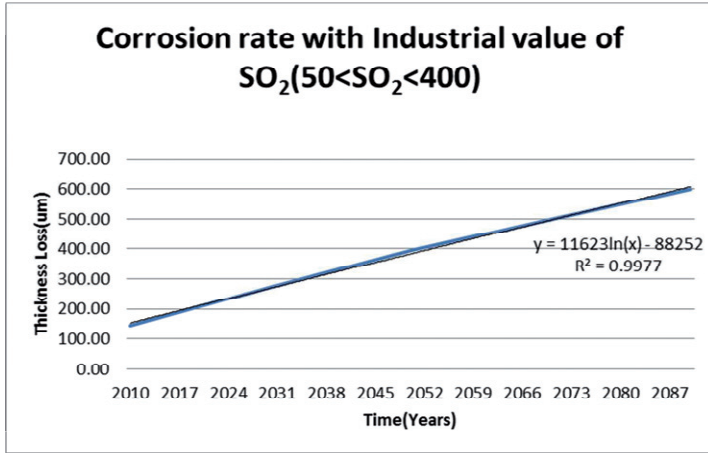


Figure 4.18 Corrosion rate for Industrial environment

DISCUSSION

From both the table and the figures, it is shown that sulphur dioxide corrosion is much higher for industrial area than in rural environment. The effect is therefore a higher thickness loss in the industrial area than in the rural. The rate of corrosion is shown to be 1.17µm/a, 2.58 µm/a and 5.68 µm/a for rural, urban and industrial areas respectively. This shows that SO₂ corrosion rate compared for rural to industrial is approximately five times while urban compared to industrial and rural compared to urban rate is slightly above two times for each.

4.6.2.3 DEPTH OF CORROSION

Steel corrosion rate with time for outdoor exposure is not constant. From ISO 9224, it is shown to decrease with exposure by the relation:

$$D = r_{\text{corrosion}} * t^{Ab} \quad \dots \quad \dots \quad \dots \quad \dots \quad \dots \quad \dots \quad \dots \quad \dots \quad \dots \quad 4.10$$

Table 4.12 Depth of corrosion penetration for various environment

Year	Corrosion Rate($r_{\text{corrosion}}$)- μm			$r_{\text{corrosion}}$ ($5 < \text{SO}_2 < 100 \mu\text{m}$)	$r_{\text{corrosion}}$ ($50 < \text{SO}_2 < 400 \mu\text{m}$)	Exposure Time(t)	Environment Factor(b)	Depth of corrosion penetration(mm)						
	Low	Average	High (Rural)					Low	Average	High(Rural)	Urban	Industrial		
2090	2050	2010												
109.4	56.16	1.93												
146.6	88.54	29.31												
182.9	119.9	55.68												
275.7	173.6	69.55												
604.9	380.3	151.3												
120	120	120												
0.026	0.026	0.026												
0.124	0.064	0.002												
0.166	0.1	0.033												
0.207	0.136	0.063												
0.312	0.197	0.079												
0.685	0.431	0.171												

4.7

STAGE TWO ANALYSIS:

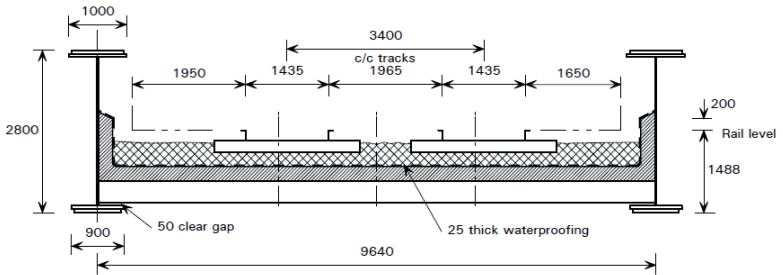
EFFECT OF CLIMATE CHANGE ON STRUCTURES

4.8 IMPACT ON A RAILWAY BRIDGE STRUCTURE

The following are the analysis carried out to determine the effect of material loss on the railway bridge structure. The worked example is of a twin-track bridge spanning 36m as in SCI Publication P318, ILES (2006). The bridge is square at its ends and the slab is wholly on top of the cross girders.

General arrangement

Cross section



Arrangement of doublers and web stiffeners

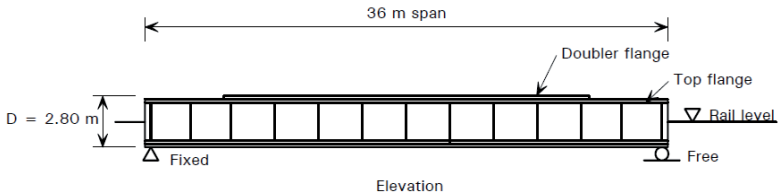


Figure 4.19 show the cross-section arrangement of the bridge

DESIGN PARAMETERS

The design is for 2 standard gauge tracks on straight alignment, track speed up to 160 km/h. Access walkway is provided on one side of the track and a continuous position of safety on the other side. The track is located with approximately 100 mm clearance between the outer edges of the walkway and the inner edges of the top flange, to allow for possible future realignment of the track.

Heavy traffic, 27 × 106 tonnes/annum was used for the analysis. Grade S355 steel and grade C40 reinforced concrete was used.

Loading

	Nominal		ULS		SLS	
	<u>kN/m</u>	<u>Factor</u>	<u>Load</u>	<u>Factor</u>	<u>Load</u>	
DEAD LOAD						
Main girder 0.267 m ² × 77 kN/m ³ plus 10%	22.61	1.0	24.87	1.00	22.61	
Cross girders 2.04 kN/m × 4.80 m / 3.0 m crs	6.53	1.10	7.18	1.00	6.53	
Slab 4.8 m × 0.25 m × 25 kN/m ³	30.00	1.20	36.00	1.00	30.00	
Haunch 0.96 m × 0.25 m × 25 kN/m ³	6.00	1.20	7.20	1.00	6.00	
Ballast 4.525 m × 0.49 m × 21 kN/m ³	46.56	1.75	81.48	1.20	55.87	
Track 2No × 2.0 kN/m × (5.07/9.64)	2.10	1.20	2.52	1.00	2.10	
Waterprfg (4.8+0.89 m) × 0.025 m × 24 kN/m ³	3.41	1.75	5.97	1.00	3.41	
Services Say	0.80	1.20	<u>0.96</u>	1.00	<u>0.80</u>	
			166.18		127.32	

Track position, relative to girders

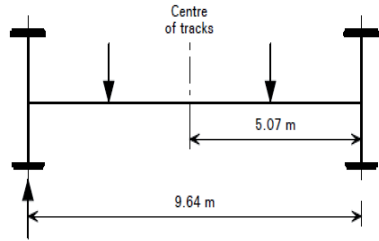


Figure 4.20 show track position for the girder

Nominal	ULS	SLS
kN/m	Factor	Factor

LIVE LOAD

EUDL 2 tracks $\times 4162 \text{ kN}/36\text{m} \times (5.07/9.64)$	121.68	1.40	170.35	1.1	133.85
Nosing (EUDL) $100 \text{ kN} \times 2/36\text{m} \times 1.338/9.64$	0.77	1.40	1.08	1.1	0.85
Walkway (far) $5 \text{ kN}/\text{m}^2 \times 0.7 \text{ m} \times 1.05/9.64$	0.38	1.50	<u>0.57</u>	1.0	<u>0.38</u>
			172.00		135.08

BENDING MOMENTS

ULS Dead load	$166.18 \times 36^2/8$	26920kNm
ULS Live load	$172.00 \times 36^2/8$	<u>27860kNm</u>
		54770kNm
SLS Dead load	$127.32 \times 36^2/8$	20630 kNm
SLS live load	$135.08 \times 36^2/8$	<u>21880 kNm</u>
		42500 kNm

Main girder - section properties

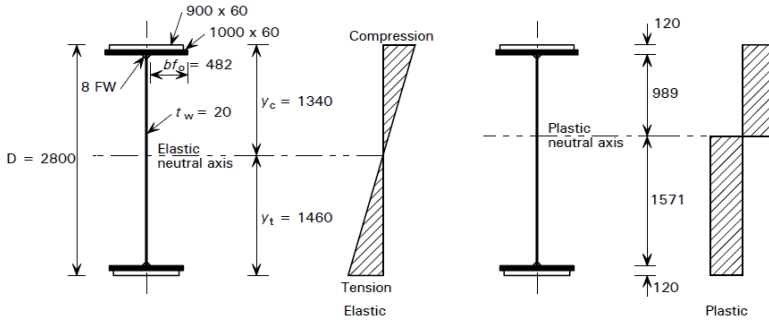


Figure 4.21 show girder section properties

Girder make-up

		yield strength (p_y)
Doubler	900 × 60 mm	335 N/mm ²
Top flange	1000 × 60 mm	335 N/mm ²
Web	2560 × 20 mm	345 N/mm ²
Bottom flange	900 × 60 mm	335 N/mm ²
Bottom doubler	800 × 60 mm	335 N/mm ²

Elastic properties for vertical bending

The second moment of area is calculated as follows:

$$I_{XX} = [(1 \cdot 0.06^3)/12 + (1 \cdot 0.06 \cdot 1.25^2)] + [(0.9 \cdot 0.06^3)/12 + (0.9 \cdot 0.06 \cdot 1.37^2)] + [(0.9 \cdot 0.06^3)/12 + (0.9 \cdot 0.06 \cdot 1.31^2)] + [(0.8 \cdot 0.06^3)/12 + (0.8 \cdot 0.06 \cdot 1.43^2)] + (0.02 \cdot 2.56^3)/12$$

$$I_{XX} = 0.4141 \text{ m}^4$$

Area A, is obtained using the following format:

$$A = 0.9 \cdot 0.06 + 1.0 \cdot 0.06 + 2.56 \cdot 0.02 + 0.9 \cdot 0.06 + 0.8 \cdot 0.06$$

$$A = 0.2672 \text{ m}^2$$

The elastic modulus is estimated from

$Z = I_{xx}/y$ for the doublers, top and bottom flanges as shown below.

$$Z_{tfd} = 0.3091 \text{ m}^3 \quad y_{bfi} = 1.460 \text{ m}$$

$$Z_{tf} = 0.3236 \text{ m}^3 \quad y_{tft} = 1.340 \text{ m}$$

$$Z_{bf} = 0.2957 \text{ m}^3$$

$$Z_{bfd} = 0.2836 \text{ m}^3$$

Plastic properties

$$Z_{pe} = M_{pe}/335 = 0.3212 \text{ m}^3 \quad y_{bfi} = 1.691 \text{ m} \quad y_{tft} = 1.109 \text{ m}$$

$M_{pe} = 107600 \text{ kNm}$ (based on yield strengths appropriate to element thicknesses) and determined as follows:

The design strength of steel reduced by appropriate partial factors, is p_y/γ_s , where $\gamma_s = 1.05 \times 1.1$ and p_y are listed above as yield strength according to BS 5400-3

$$M_{pl} = R_{fb} (D - y_p) + R_{ft} \cdot y_p + R_w y_p^2 / 2d + R_w (d - y_p)^2 / 2d$$

Tensile Resistance of Bottom Flange

$$\begin{aligned} R_{fb} + R_{fbd} &= 60 \times 900 \times (335 / (1.05 \times 1.1)) \times 10^{-3} + 60 \times 800 \times \\ & (335 / (1.05 \times 1.1)) \times 10^{-3} \\ &= 15714 + 13968 = 29682 \text{ kN} \end{aligned}$$

Tensile Resistance of Top Flange

$$\begin{aligned} R_{ft} + R_{ftd} &= 60 \times 1000 \times (335 / (1.05 \times 1.1)) \times 10^{-3} \\ &+ 60 \times 900 \times (335 / (1.05 \times 1.1)) \times 10^{-3} \\ &= 17460 + 15714 = 33174 \text{ kN} \end{aligned}$$

Tensile Resistance of web

$$\begin{aligned} R_w &= dt_w p_y = (2800 - 240) \times 20 \times (345 / (1.05 \times 1.1)) \times 10^{-3} \\ &= 15360 \text{ kN} \end{aligned}$$

Check if: $R_{ft} + R_w \geq R_{fb}$: PNA lies in web

$$33174 + 15360 > 29682$$

$$\begin{aligned} \text{PNA: } y_p &= ((2800-240)/2) \times ((29682-33174+15360)/15360) \\ &= 989 \text{ mm} \end{aligned}$$

Therefore, plastic moment capacity, is

$$\begin{aligned} M_{pe} &= 29682(2800-1109) \times 10^{-3} + 33174 \times 1109 \times \\ &10^{-3} + ((15360/2) \times (989^2/2500)) \times 10^{-3} + ((15360/2) \times (2500- \\ &989)^2) \times 10^{-6} \\ &= 107600 \text{ kNm} \end{aligned}$$

Shape limitations

$b_{f0} = 482 \text{ mm} > 7t_{f0} \sqrt{(355/\sigma_y)} = 420 \times 1.029 = 432 \text{ mm}$ Non-compact according to BS 5400-3, 9.3.7.3.1

Clear web depth = 2544 mm $m = (1109 - 128)/2544 = 0.3856$

Limit for compact web: $34 t_w / m \sqrt{(355/\sigma_{yw})}$
 $= 680 \times 1.014 / 0.3856 = 1788 \text{ mm}$ Non-compact according to BS 5400-3, 9.3.7.2

Effective sections

Web: $y_c/t_w \sqrt{\sigma_{yw}/355} = (1460 - 120)/20 \sqrt{(345/355)} = 60 < 68$ Web fully effective according to BS 5400-3, 9.4.2.5.1

Slenderness of main girders

$l_e = k_2 k_3 k_5 l_1$ to BS 5400-3, 9.6.4.1.3

$$l_1 = (EI_c / R \delta_R)^{0.25} \quad 9.6.4.1.1.2$$

I_c for a 1000 × 60 flange and 900 × 60 doubler = 0.008645 m⁴

$$l_1 = (205 \times 10^6 \times 0.008645 \times 3.0 \times 0.0001453)^{0.25} = 5.272 \text{ m}$$

$$X = l_1 / (\sqrt{2EI_c} \delta_{e,\max})$$

$$X = 5.272^3 / (\sqrt{2} \times 205 \times 10^6 \times 0.00865 \times 0.0000686)$$

$$= 0.852$$

$$k_5 = 2.22 + 0.69 / (X + 0.5)$$

$$= 2.730$$

$k_2 = 1.0$ (load on girder at bottom flange level)

$k_3 = 1.0$ (no rotation restraint in plan at supports)

$$l_e = 1.0 \times 1.0 \times 2.730 \times 5.272 = 14.39 \text{ m}$$

For slenderness of U-frames, λ_{LT} is given by:

$$\lambda_{LT} = l_e / r_{yc} \text{ according to BS 5400-3, 9.7.2}$$

The value of r_{yc} is that for the top flange plus one third of the depth of the web.

For that section:

$$I_c = 0.008645 \text{ m}^4$$

$$A = 0.131$$

$$r_{yc} = 0.257 \text{ m}$$

Hence

$$\lambda_{LT} = 14.39 / 0.257 = 56.0$$

Moment of resistance of main girder

Consider buckling mode:

$$L / l_e = 36 / 14.39 = 2.50, \text{ Hence there will be two half waves and } l_w$$

$$= 18.0 \text{ m}$$

For input to Figure 11 : BS 5400-3

$$\lambda_{LT} \sqrt{[(\sigma_{yc} / 355) (M_{ult} / M_{pe})]} = 56.0 \sqrt{(335 / 355) (95010 / 107600)}$$

$$= 52.6$$

$$l_e / l_w = 14.39 / 18.00 = 0.80$$

From Figure 11a $M_R / M_{ult} = 0.698$

Hence $M_R = 0.698 \times 95010 = 66320 \text{ kNm}$

$M_D = M_R / (\gamma_m \gamma_{fs}) = 66320 / (1.05 \times 1.1) = 57420 \text{ kNm}$

This is slightly more than the applied moment and will probably be satisfactory.

Check on dynamic performance

Dead load 127.5 kN/m (nominal DL + 100 mm extra ballast)

Deflection = $5 \times 127.5 \times 36^4 / (384 \times 205 \times 10^6 \times 0.414) \times 1000 = 32.8 \text{ mm}$

This value is below the upper limit for a span of 36 m in Figure 5 of UIC 776-2R

Live load (Nominal value, 2 tracks) 121.6 kN/m

Deflection = $5 \times 121.6 \times 36^4 / (384 \times 205 \times 10^6 \times 0.414) \times 1000 = 31.3 \text{ mm}$

Span/deflection = $36000 / 31.3 = 1150.2$

This ratio is better than the limit of 800 in Table 4 of UIC 776-3R for a single deck

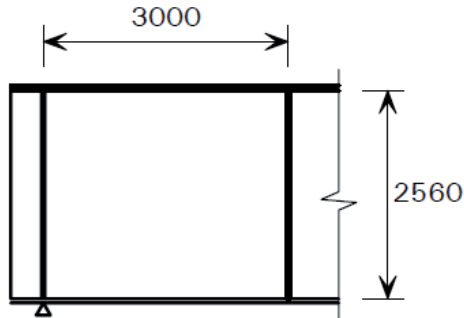
Shear resistance

Loading at ULS

		Shear (kN)
Dead load	$166.18 \times 36/2$	2991
Live load (RU EUL)	$2 \times (2094 \times 1.4) \times 5.07/9.64$	3084
Nosing	$100 \times 1.4 \times 1.338/9.64$	<u>40</u>
		6115

Clear Depth of web $d_{we} = 2560 \text{ mm}$

Spacing of stiffeners $a = 3000$ mm



Flanges are parallel and straight, so use clause

9.9.2.2 of BS 5400-3 according to cl 9.9.2.1

$$\phi = 3000/2560 = 1.172$$

$$\begin{aligned} \lambda &= d_{we}/t_w \sqrt{\sigma_{yw}/355} \\ &= 2560/20 \sqrt{345/355} \\ &= 126 \end{aligned}$$

For $m_{fw} = 0$, Figure 12 gives $\tau_1/\tau_u = 0.609$

Effective width of flange for m_{fw} (bottom flange is smaller if no doubler) according to cl 9.9.2.2

$$\begin{aligned} b_{fe} &= \text{is the lesser of } 10 t_f \sqrt{355/\sigma_{yf}} = 10 \times 60 \sqrt{355/335} \\ &= 618 \text{ mm} \end{aligned}$$

and $b_f/2 = 450$ mm

Hence $b_{fe} = 450$ mm

$$\begin{aligned} m_{fw} &= \sigma_{yf} b_{fe} t_f^2 / 2\sigma_{yw} d_{we}^2 t_w \\ &= 335 \times 450 \times 60^2 / (2 \times 345 \times 2560^2 \times 20) \\ &= 0.00600 \end{aligned}$$

For $m_{fw} = 0.005$, Figure 13 gives $\tau_1/\tau_u = 0.695$ and for $m_{fw} = 0.0105$,

Figure 14

gives $\tau_1/\tau_u = 0.790$

So for $m_{fw} = 0.00600$ $\tau_1/\tau_u = 0.714$

$$\tau_u = 345 / 3 = 199 \text{ N/mm}^2$$

$$\tau_l = 0.714 \times 199 = 142 \text{ N/mm}^2$$

$$VD = [t_w(d_w - h_n) / (\gamma_m \gamma_{f3})] \tau_l$$

$$= [20 \times (2560 - 0) / 1.05 \times 1.1] \times 142 \times 10^{-3}$$

$$= 6294 \text{ kN} \quad \text{according to cl 9.9.2.2}$$

The same procedure is repeated for all the thickness losses as shown in the table below.

Table 4.13 Thickness losses analysed

Year	Thickness Loss for the Analysis(mm)		
	Rural	Urban	Industrial
2010	0.10	0.10	0.20
2050	0.15	0.20	0.48
2090	0.21	0.30	0.70

However, for brevity only the thickness loss for 0.10mm for rural area in 2010 is repeated as shown below

Thickness loss @ 0.10mm for Year 2010 Girder make-up

		yield strength (p_y)
Doubler	899.8 × 60 mm	335 N/mm ²
Top flange	999.8 × 59.8 mm	335 N/mm ²
Web	2560.2 × 19.8 mm	345 N/mm ²
Bottom flange	899.8 × 59.8 mm	335 N/mm ²
Bottom doubler	799.8 × 60 mm	335 N/mm ²

Elastic properties for vertical bending

The second moment of area is calculated as follows:

$$I_{xx} = [(0.9998 \cdot 0.0598^3)/12 + (0.9998 \cdot 0.0598 \cdot 1.2501^2)] + \\ [(0.8998 \cdot 0.0598^3)/12 + (0.8998 \cdot 0.0598 \cdot 1.3701^2)] \\ + [(0.898 \cdot 0.06^3)/12 + (0.8998 \cdot 0.06 \cdot 1.31^2)] + [(0.7998 \cdot 0.06^3)/12 \\ + (0.7998 \cdot 0.06 \cdot 1.43^2)] + (0.0198 \cdot 2.5602^3)/12 \\ I_{xx} = 0.4129 \text{ m}^4$$

Area A, is obtained using the following format:

$$A = 0.9998 \cdot 0.0598 + 0.8998 \cdot 0.0598 + 2.5602 \cdot 0.0198 + 0.8998 \cdot 0.06 \\ + 0.7998 \cdot 0.06 \\ A = 0.2662 \text{ m}^2$$

The elastic modulus is estimated from

$Z = I_{xx}/y$ for the doublers, top and bottom flanges as shown below.

$$Z_{tfd} = 0.3079 \text{ m}^3 \quad y_{bfl} = 1.458 \text{ m} \\ Z_{tr} = 0.3223 \text{ m}^3 \quad y_{trl} = 1.341 \text{ m} \\ Z_{bf} = 0.2954 \text{ m}^3 \\ Z_{bfd} = 0.2832 \text{ m}^3$$

Plastic properties

$$Z_{pe} = M_{pe}/335 = 0.3202 \text{ m}^3 \quad y_{bfl} = 1.6934 \text{ m} \quad y_{trl} = 1.1066 \text{ m}$$

$M_{pe} = 107300 \text{ kNm}$ (based on yield strengths appropriate to element thicknesses) and determined as follows:

The design strength of steel reduced by appropriate partial factors, is p_y/γ_s , where $\gamma_s = 1.05 \times 1.1 \approx 1.15$ and p_y are listed above as yield strength according to BS 5400-3

$$M_{pl} = R_{fb} (D - y_p) + R_{ft} \cdot y_p + R_w y_p^2/2d + R_w (d - y_p)^2/2d$$

Tensile Resistance of Bottom Flange

$$\begin{aligned}R_{fb} + R_{fbd} &= 59.8 \times 899.8 \times (335 / (1.15)) \times 10^{-3} \\ &\quad + 60 \times 799.8 \times (335 / (1.15)) \times 10^{-3} \\ &= 15658 + 13965 = 29623 \text{ kN}\end{aligned}$$

Tensile Resistance of Top Flange

$$\begin{aligned}R_{ft} + R_{ftd} &= 59.8 \times 999.8 \times (335 / (1.15)) \times 10^{-3} \\ &\quad + 60 \times 899.8 \times (335 / (1.15)) \times 10^{-3} \\ &= 17398 + 15711 = 33109 \text{ kN}\end{aligned}$$

Tensile Resistance of web

$$\begin{aligned}R_w = dt_w p_y &= (2800 - 240) \times 19.8 \times (345 / (1.15)) \times 10^{-3} \\ &= 15206 \text{ kN}\end{aligned}$$

Check if: $R_{ft} + R_w \geq R_{fb}$: PNA lies in web

$$33109 + 15206 > 29623$$

$$\begin{aligned}\text{PNA: } y_p &= ((2800 - 240) / 2) \times ((29623 - 33109 + 15206) / 15206) \\ &= 987 \text{ mm}\end{aligned}$$

Therefore, plastic moment capacity, is

$$\begin{aligned}M_{pe} &= 29623(2800 - 1107) \times 10^{-3} + 33109 \times 1107 \times \\ &\quad 10^{-3} + ((15206 / 2) \times (987^2 / 2500)) \times 10^{-3} + ((15206 / 2) \times (2500 - \\ &\quad 987)^2) \times 10^{-6} \\ &= 107200 \text{ kNm}\end{aligned}$$

M_{pe} 107200 kNm (based on yield strengths appropriate to element thicknesses)

Shape limitations

$b_{f0} = 482 \text{ mm} > 7t_{f0} \sqrt{(355 / \sigma_y)} = 420 \times 1.029 = 431 \text{ mm}$ Non-compact according to BS 5400-3, 9.3.7.3.1

Clear web depth = 2544.2 mm $m = (1109 - 127.8)/2544 = 0.3845$

Limit for compact web: $34 t_w/m\sqrt{(355/\sigma_{yw})}$

= $680 \times 1.014 / 0.3845 = 1776$ mm Non-compact according to
BS 5400-3, 9.3.7.2

Effective sections

Web: $y_c/t_w\sqrt{\sigma_{yw}/355} = (1458.8 - 119.8)/19.8\sqrt{(345/355)} = 66.7 < 68$

Web fully effective according to BS 5400-3, 9.4.2.5.1

Slenderness of main girders

Assume cross girder restrain not corroded

$l_e = k_2 k_3 k_5 l_1$ to BS 5400-3, 9.6.4.1.3

$l_1 = (EI_{dLR}\bar{\sigma}_R)^{0.25}$ 9.6.4.1.1.2

I_c for a 999.8×59.8 flange and 899.8×60 doubler = 0.008623 m^4

$l_1 = (205 \times 10^6 \times 0.008623 \times 3.0 \times 0.0001453)^{0.25} = 5.268 \text{ m}$

$X = l_1 / (\sqrt{2EI_c} \bar{\delta}_{e,\max})$

$X = 5.272^3 / (\sqrt{2 \times 205 \times 10^6 \times 0.00862 \times 0.0000686})$
= 0.853

$k_5 = 2.22 + 0.69/(X+0.5)$
= 2.730

$k_2 = 1.0$ (load on girder at bottom flange level)

$k_3 = 1.0$ (no rotation restraint in plan at supports)

$l_e = 1.0 \times 1.0 \times 2.730 \times 5.268 = 14.39 \text{ m}$

For slenderness of U-frames, λ_{LT} is given by:

$\lambda_{LT} = l_e/r_y$ according to BS 5400-3, 9.7.2

The value of r_{yc} is that for the top flange plus one third of the depth of the web.

For that section:

$$I_c = 0.008623 \text{ m}^4$$

$$A = 0.131 \text{ m}^2$$

$$r_{yc} = 0.257 \text{ m}$$

Hence

$$\lambda_{LT} = 14.39/0.257 = 56.0$$

Moment of resistance of main girder

Consider buckling mode:

$L/l_e = 36/14.39 = 2.50$, Hence there will be two half waves and $l_w = 18.0 \text{ m}$

For input to Figure 11 : BS 5400-3

$$\lambda_{LT} \sqrt{[(\sigma_{yc}/355)(M_{ult}/M_{pe})]} = 56.0 \sqrt{(335/355)(95010/107200)} \\ = 51.21$$

$$l_e/l_w = 14.39/18.00 = 0.80$$

From Figure 11a $M_R/M_{ult} = 0.71$

Hence $M_R = 0.71 \times 95010 = 67457 \text{ kNm}$

$$M_D = M_R/\gamma_m \gamma_{f3} = 67457/(1.05 \times 1.1) = 58404 \text{ kNm} > 54770 \text{ kNm}$$

This is slightly more than the applied moment and will probably be satisfactory.

Check on dynamic performance

Dead load 127.5 kN/m (nominal DL + 100 mm extra ballast)

$$\text{Deflection} = 5 \times 127.5 \times 36^4 / (384 \times 205 \times 10^6 \times 0.4129) \times 1000 = 32.94 \text{ mm} \\ < 45 \text{ mm}$$

This value is below the upper limit for a span of 36 m in Figure 5 of UIC 776-2R

Live load (Nominal value, 2 tracks) 121.6 kN/m

$$\text{Deflection} = 5 \times 121.6 \times 36^4 / (384 \times 205 \times 10^6 \times 0.4129) \times 1000 = 31.42 \text{ mm} \\ < 45 \text{ mm}$$

Span/deflection = $36000/31.42 = 1145.76 > 800$

This ratio is better than the limit of 800 in Table 4 of UIC 776-3R for a single deck

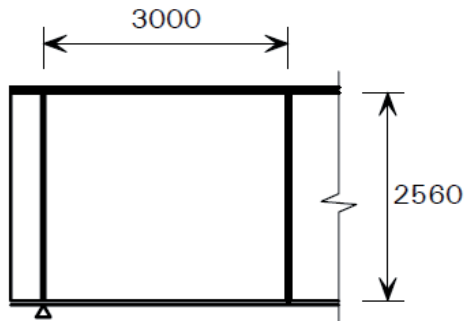
Shear resistance

Loading at ULS

		Shear (kN)
Dead load	$166.18 \times 36/2$	2991
Live load (RU EUL)	$2 \times (2094 \times 1.4) \times 5.07/9.64$	3084
Nosing	$100 \times 1.4 \times 1.338/9.64$	<u>40</u>
		6115

Clear Depth of web $d_{we} = 2560$ mm

Spacing of stiffeners $a = 3000$ mm



Flanges are parallel and straight, so use clause 9.9.2.2 of BS 5400-3 according to cl 9.9.2.1

$$\varphi = 3000/2560.2 = 1.172$$

$$\begin{aligned} \lambda &= d_{we}/t_w \sqrt{\sigma_{yw}/355} \\ &= 2560.2/19.8 \sqrt{345/355} \\ &= 127.46 \end{aligned}$$

For $m_{fw} = 0$, Figure 12 gives $\tau_1/\tau_u = 0.62$

Effective width of flange for m_{fw} (bottom flange is smaller if no doubler) according to cl 9.9.2.2

$$b_{fe} = \text{is the lesser of } 10 t_f \sqrt{355} / \sigma_{yf} = 10 \times 59.8 \sqrt{355} / 335$$

$$= 616 \text{ mm}$$

$$\text{and } b_f / 2 = 449.9 \text{ mm}$$

$$\text{Hence } b_{fe} = 449.9 \text{ mm}$$

$$m_{fw} = \sigma_{yf} b_{fe} t_f^2 / 2 \sigma_{yw} d_{we}^2 t_w$$

$$= 335 \times 449.9 \times 59.8^2 / (2 \times 345 \times 2560.2^2 \times 19.8)$$

$$= 0.00601$$

For $m_{fw} = 0.005$, Figure 13 gives $\tau_I / \tau_U = 0.695$ and for $m_{fw} = 0.0105$, Figure 14

$$\text{gives } \tau_I / \tau_U = 0.790$$

$$\text{So for } m_{fw} = 0.00600 \quad \tau_I / \tau_U = 0.714$$

$$\tau_U = 345 / 3 = 199 \text{ N/mm}^2$$

$$\tau_I = 0.714 \times 199 = 142 \text{ N/mm}^2$$

$$VD = [t_w (d_w - h_h) / \gamma_m \gamma_{f3}] \tau_I$$

$$= [19.8 \times (2560.2 - 0) / 1.05 \times 1.1] \times 142 \times 10^{-3}$$

$$= 6232 \text{ kN} > 6115 \text{ kN} \quad \text{according to cl 9.9.2.2}$$

The result of other calculations are as shown in table 4.14 below and a plot of the effect of thickness loss on moment resistance, shear resistance and deflection in the figures.

Table 4.14 show calculated resistances for various corrosion types

Case	Type of Corrosion	Years	Moment Resistance, M_D – kNm		Shear Resistance, V_D -kN		Deflection, δ (mm)	
			Load	Resistance	Load	Resistance	Load	Resistance
Case1	Normal section as Designed		X		x		x	
	2010 - No corrosion	2010	54770	57420	6115	6294	45	31.3
Case2	Full section corroded (Rural)		X		x		x	
Case 2a	2010 high corrosion depth	2010	54770	58404	6115	6232	45	31.42
Case 2b	2050 high corrosion depth	2050	54770	58322	6115	6201	45	31.46
Case 2c	2090 high corrosion depth	2090	54770	58240	6115	6164	45	31.5
Case3	Full section corroded (Urban)		X		x		x	
Case3a	2010 high corrosion depth	2010	54770	58404	6115	6232	45	31.42
Case3b	2050 high corrosion depth	2050	54770	58240	6115	6164	45	31.5
Case 3c	2090 high corrosion depth	2090	54770	57911	6115	6120	45	31.58
Case4	Full section corroded (Industrial)		X		x		x	
Case 4a	2010 high corrosion depth	2010	54770	58240	6115	6164	45	31.5
Case 4b	2050 high corrosion depth	2050	54770	58158	6115	6039	45	31.68
Case 4c	2090 high corrosion depth	2090	54770	56677	6115	5882	45	31.9

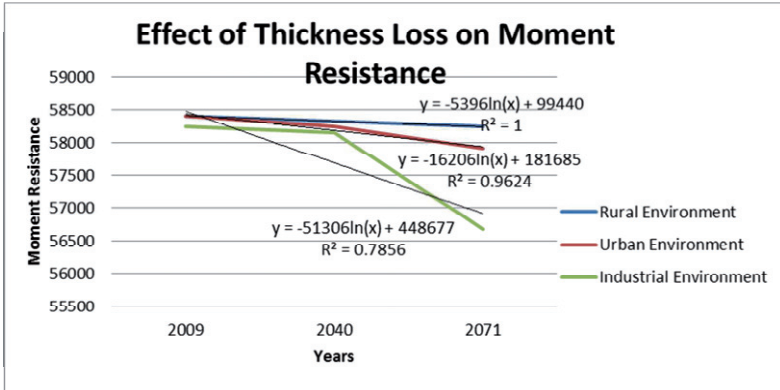


Figure 4.22 Effect of thickness loss on moment resistance of bridge girder

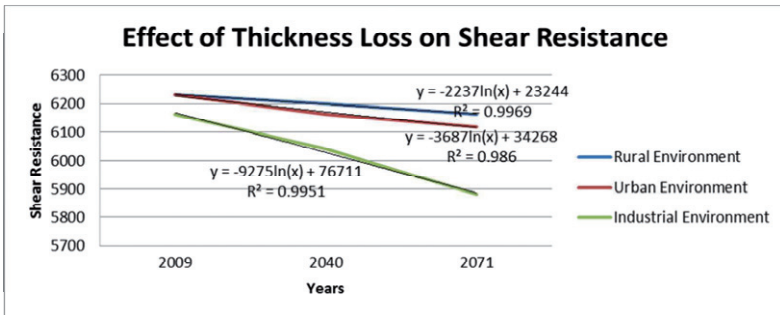


Figure 4.23 Effect of thickness loss on shear resistance of bridge girder

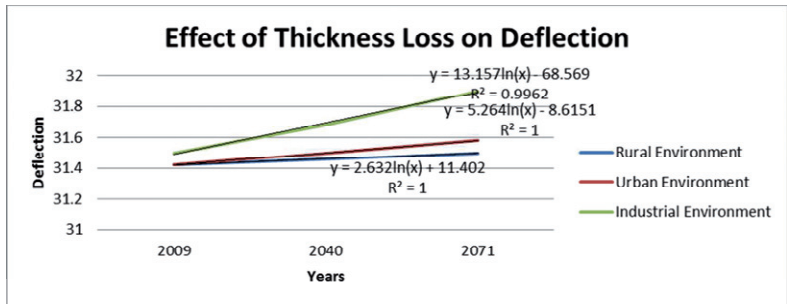


Figure 4.24 Effect of thickness loss on deflection of bridge girder

DISCUSSION

From the results shown in table above and reflected in the figures 4.22 - 4.24, thickness loss due to corrosion of steel structure caused by climate change has long term impact on the effectiveness of the structure to carry the design load.

It is obvious that the moment resistance decreases with time depending on the location of the structure. The analysis shows that the rate of decrease of moment resistance is 0.3% for rural area, 0.9% for urban area and 3% for industrial environment. For industrial locations, the rate of fall of moment resistance increases faster after 40years, a period of stable decrease as the top flange deteriorate.

The shear resistance fall is sharper for all environments, as the web is the load carrying member in the girder with small thickness. For the rural area the decrease in shear resistance is slightly above 1%, while the urban and industrial areas is 1.8% and 4.6% respectively.

This will justify the need to increase the thickness of the web and reduce the spacing of the stiffeners.

From figure 4.24 the deflection of the girder increases with time and location of the structure. Deflection is more with industrial location and least in rural environment as the analysis has shown, 0.18% for rural area over time, 0.36% for urban environment and 0.89% for industrial location.

4.9 CHAPTER SUMMARY

The chapter discussed the results obtained from various analysis carried out in two stages. In stage one, emission scenarios for climate change were noted; while the pollutants that cause global warming was also discussed as it concerns their change with time.

Using the determined dose-response function of air pollutant and climate parameters, thickness loss for a steel bridge structure was analyzed.

The second stage involves the check of the effect of thickness loss on moment resistance, shear resistance and deflection of the analyzed bridge as shown. Results obtained indicate that while the moment and shear force resistance of the structure is decreasing with thickness loss over time, deflection is increasing. Also, doubler plates are used to increase the flange thickness required to check for fatigue in railway steel bridge beams.

CHAPTER FIVE

SUMMARY, CONCLUSIONS, AND FUTURE WORK

5.1 SUMMARY

In chapter one, the subject of impact of climate change on the rate of deterioration of existing structures was introduced. It also looked at the significance and objective of the study while noting past research on the subject.

The general objective of this research is to study the factors that actually have impact on the service life existence and progress of deterioration of structures exposed to atmospheric weathering.

Detailed literature review to determine what is known and gaps in knowledge followed in chapter two. The chapter reviewed the current efforts made to study the impact of natural and anthropogenic factors on climate and the effect of change in climate and air quality on human. It was observed from studies that the climate/weather will continue to change due to the damaging influence of human's activities on the earth. Though the factors that influence climate change is known, their interaction with the earth is difficult to estimate.

Various building materials affected by climate change were identified with their impact noted. The impact of climate change was observed to be more noticeable in the urban areas than in the rural setting due to the effect of industrial gases and other anthropogenic effect in the atmosphere.

In chapter three, the method of analysis was considered. Two stages were involved, first is the determination of the rate of material loss through the appropriate dose-response function and the second stage is the use of the calculated thickness loss to determine the bending resistance, shear resistance and deflection of the single span railway bridge.

Chapter four discussed the results obtained from various calculations carried out in the two stages of analysis. In stage one, emission scenarios for climate change were noted; while the pollutants that cause global warming was also discussed as it concerns their change with time. Using the determined dose-response function of air pollutant and climate parameters, thickness loss for a steel bridge structure was analyzed.

From the result obtained in first stage, a check on the effect of thickness loss on moment resistance, shear resistance and deflection of the analyzed bridge is conducted. Results obtained indicate that while the moment and shear force resistance of the structure is decreasing with thickness loss, deflection is increasing.

5.2 CONCLUSIONS AND RECOMMENDATIONS

Guildford, a borough in the southeast of England is likely to witness an increase in temperature in the range of 2°C - 6°C by 2100 especially in the summer.

- The pollution by SO₂ is projected to fall within the corresponding period as increased emission control measures take effect.

- From impact study it is shown that the rainfall patterns will change, bringing drier summer and wetter winters
- Carbon dioxide which is a major cause of greenhouse effect is estimated to increase under all emission scenarios because of increased use of various energy resources.

All other objectives as stated are determined as follows:

- The ISO 9223 dose-response function was determined as the most suitable. The function was noted to be an approximation of the average of all the known functions. Also the climate parameters and air pollutants reflected the conditions obtainable in rural, urban and Industrial cities of UK.
- Estimate shows that there is objectionable thickness loss within the 120years life span of the structures under the ISO 9223 categorization for urban and industrial environment.
- The moment resistance for the designed structure shows a decrease of 0.3% for rural area, 0.9% for urban area and 3% for industrial environment. Shear resistance decrease is 1.1% for rural, 1.8% for urban and 4.6% for industrial areas.
- From the various dose-response functions by different researchers an upper and lower bound was established. The average dose-response function on this has a function $y = 3006\ln(x) - 22834$ with a coefficient $R^2 = 0.96$
- The result of the parametric analysis has shown that the presence of SO_2 , a pollutant resulting from industrial activities and high relative humidity based on climate factors affects thickness loss. In this regard a 10% increase in the two factors will cause a 5% increase in thickness loss for SO_2 and 15% thickness loss for relative humidity.

5.3 FUTURE WORK

- One of the limitations for the achievement of the objectives of this work is the sourcing of data for the study location Guildford. Available long term records are mainly for London, hence the use in the work
- A study of the correlation of London climate and pollution records and the existing Guildford information will help to improve the work
- Further improvement could be made by undertaking a long term dose-response study of the project location to confirm the classification of the area
- Finally, it is hoped that another researcher may look at the fatigue behaviour of the structure under the same condition.

REFERENCES

A Special Report of IPCC Working Group III, (2000). Summary for policymakers on Emissions Scenarios. Pub. for the Intergovernmental Panel on Climate Change.

An Assessment of the Intergovernmental Panel on Climate Change. (2007). Climate change 2007: Synthesis reports. IPCC Plenary XXVII (Valencia, Spain, 12-17 November 2007

Arroyave, C. and Morcillo, M. (1995). The Effort of Nitrogen Oxide in Atmospheric Corrosion of Metals; Corrosion Science, Vol. 37 No. 2 pg. 293-305.

Ayoade, J.O. (2004), "Introduction to Climatology for the Tropics" (2nd Ed.), Spectrum Books Ltd., Nigeria

Bach, W. (1972). Atmospheric Pollution New York: McGraw-Hill.

Banks, W.B. and Evans, P.D. (1984). Degradation of Wood Surfaces by Water. Proc. 18th Annual Meeting, International Research Group on Wood Preservation, Stockholm.

Barry, R.G. and Chorley, R.J. (1976), Atmosphere, Weather and Climate (3rd Ed) London: Methuen.

Bartonj, K. and Cherny, M. Zashch, Met. 1980, Vol. 16, No. 4 Pg. 387.

Brimblecombe, P; Grossi, C.M. (2007); Damage to Buildings from Future Climate and Pollution. APT Bulletin, Vol. 38, P 13-18.

Brimblecombe P., Grossi, C.M. (2008), "Millenium-long Recession of limestone Facades in London", Environ Geol. 56: Pg 463-471.

BS EN ISO 9223:2012. Corrosion of metals and alloys - Corrosivity of atmospheres - Classification, determination and estimation. The British Standard Institute.

BS 5400-3:2000. Steel, concrete and composite bridges-Part 3: Code of practice for design of steel bridges. The British Standard Institute.

Burton, L et al (1978), Scope Workshop and Climate/Society Interface, Canada: Toronto.

Butlin, R. N. et al (1992b) Preliminary Results from the Analysis of Metal Samples from National Materials Exposure programme (NMEP). Atmospheric Environment 26B 199.

Cooke, R.U. and Gibbs, G. B. (1994). Crumbling Heritage? Studies of Stone Wreathing in Polluted Atmosphere, National Power Swindon.

Critchfield, H. J. (1974) General Climatology, New Jersey; Prentice-Hall Inc.

Danny Harvey, L. D. (2000), "Climate and Global Environmental Change", Pearson Edu. Ltd, UK, Pg. 9-11, Chapter 2.

DECC Statistical Release (2012). 2011 UK Greenhouse gas emissions, provisional figures and 2010 UK Greenhouse gas emissions, final figures by fuel type and end-user. Department of Energy and Climate Change, Whitehall Place, London SW1A 2AW.

Duke, R. (2011), "This Shrinking Land Climate Change and Britain's Coasts" Dundee University Press, UK.

Economic Commission for Europe (1984). Air Pollution 1 Air-Borne Sulphur, Pollution Effect and Control, Report prepared within the Framework of the Convention on Long-range Transboundary Air Pollution, UN Publication Geneva.

EternE (European Commission, 1998), "Assessment of Global Warming Damages", <http://www.externeinfo/reportex/vol7.pdf>

Feenstra, J.F. (1984), "Cultural Property and Air Pollution: Damage to Monuments, Art – Objects, Archives and Buildings due to Air Pollution", Ministry of Housing, Physical Planning and Environment, the Netherlands.

Giffiths, J.F. (1976). Climate and the Environment: The Atmospheric Impact, London: Paul Elek.

Hart, A. B. (1997), "A Risk Assessment of the Iceland area around Charmouth, West Dorset. M. Sc. Thesis, University of Portsmouth.

Hart, M. B. (Ed) 2000, "Climate: Past and Present", Geological Society Special Publication No. 181, UK, Pg 1-4.

Henriksen, J.F. and Rode, A. (1986). Proc. 10th Scandinavian Corrosion Cong., P. 39. Stockholm.

Hobbs, J.E. (1980). Applied Climatology: A Study of Atmospheric Resources. Damson, Folkestone.

Houghton, J.T. (2004). Global Warming: The Complete Briefing (3rd Ed). Cambridge University Press, Cambridge.

Hulme, M. and Kenkins, G. J. (1998), "Climate Change Scenarios for the UK. Scientific Report UKCIP Technical Report No. 1, Climate Research Unit Norwich.

Hutchinson, P. (2006). Images of England: Guildford. The History press, Gloucestershire, UK.

ILES, D.C (2004). Design Guide for Steel Railway Bridges. The Steel Construction Institute. Publication P318.

Imram Rafiq, M; Chryssanthopoulos, M.K and Onoufriou, T. (2004). Performance upgrading of concrete bridges using

proactive health monitoring methods. Reliability Engineering and System Safety 86 pp.247-256.

Kayer, J.R & Nowak, A.S. (1989). Reliability of Corroded Steel Girder Bridges. Structural Safety, vol.6, pp.53-63.

Kozłowski, R. (2007), "Climate-Induced Damage of Wood: Numerical Modelling and Direct Tracing", Contribution to the Expert's Roundtable on Sustainable Climate Management Strategies, Tenerife, Spain.

Kihira, H; Senuma, T; Tanaka, M; Nishioka, R; Yosumori, F; Sakata, Y (2005). A Corrosion Prediction Method for Weathering Steels. Corrosion Science, Vol. 47, 2377-2390.

Kucera, V. (1994). The UN ECE International Cooperative Programme on Effects on Material, Including Historic and Cultural Monuments. Report to the Working Group on Efforts within the UN ECE in Geneva, Swedish Corrosion Institute, Stockholm.

Kucera, V. et al (2005), EU5FP RTD Project: Model for Multi-Pollutant Impact and assessment of Threshold levels for cultural heritage. Multi-Assess Publishable Final Report. <http://www.corrosioninstitute.se/MULTI-ASSESS/>

Kucera, V; Tidblad, J; Kreislova, K; Knotkova, D; Faller, M; Reiss, D; Sneathlaga, R; Yates, T; Henriksen, j; Schreiner, M; Melcher, M; Ferm, M; Lefevre, R; Kobus, J. (2007). UN/ECE ICP Materials

Dose-Response Functions for the Multi-pollutant Situation. *Water Air Soil Pollution: Focus* 7: 249-258.

Lahdensivu, J., Weijo, I; Mattila, J. (2009). *Existence of Deterioration in Concrete Balconies*: Taylor and Francis Group, London, UK.

Lamb, H. H. (1995), *Climate History and the Modern World*. Routledge, London.

Land Use Consultants (2003). *Living with Climate Change in the East of England, Stage 1 Report: Guidance on Spatial Issues*. Prepared for Hertfordshire County Council on behalf of the East of England Regional Assembly and East of England Sustainable Development Roundtable.

Leuenberger – Minger, A. U; Buchmann, B; Faller, M; Richner, P; Zobeli, M. (2002). Dose-response Functions of Weathering Steel, Copper and Zinc Obtained from a Four-year Exposure Programme in Switzerland. *Corrosion Service* 44 Pg. 675-687.

Life Application Study Bible (2005), "New International Version", Tyndale House Pub. Inc. USA.

Lipfert, F. W. (1987). *Effects of Acidic Deposition on the Atmospheric Deterioration of Materials*. Material Performance, 12, National Association of Corrosion Engineers, 1987.

Lockwood, J.G. (1979), *Causes of Climate*, London: E. Arnold.

Manley G. (1974) Central England Temperature: Monthly Means 1659-1972. QJR Meteorological Soc. 100: 389-405.

Mather, J.R. (1974), Climatology: Fundamentals and Applications, New York: Mc Graw-Hill.

Maunder, W.J. (1970). The value of the Weather, London: Methuen.

McDermott, W. (1961). Air pollution and Public Health, Scientific American, 612, 49-57.

Melchers, R. (2002). Structural Reliability Analysis and prediction, 2nd Ed. John Wiley & Sons.

Mellanby, K (1988). "Air pollution, Acid Rain and the Environment", Report Number 18, Watt Committee Report: Edited.

Mikhailov, A.A. (2001). "Dose-Response Functions as Estimates of the Effect of Acid Precipitation on Material", Protection of Metals, Vol. 37 No. 4 2001, P. 8 357-366. Translated from Zashchita Metallov Vol. 37, No. 4 2001, Pp 400-410 Original Russian Text Copyright ©2001 by Mikhailov.

Misawa, T; Asami, K; Hashimoto, K; Shimodaira, S. (1974). The Mechanism of Atmospheric Rusting and the Protective Amorphous Rust on Low Alloy Steel. Corrosion. Sci – 14, 279-289.

Nakićenović, N., Davidson, O., Davis, G., Grübler, A., Kram, T., La Rovere, E., Metz, B., Morita, T., Pepper, W., Pitcher, H., Sankovski, A., Shukla, P., Swart, R., Watson, R. & Dadi, Z. 2000. *IPCC Special Report on Emission Scenarios*. Cambridge University Press, Cambridge.

Ozelton, E.C and Baird, J.A. (2008). *Timber Designers' Manuel*, 3rd Ed Revised, Blackwell Science Ltd, Oxford United Kingdom.

Park, C.H. (1999). *Time Dependent Reliability models for Steel Girder Bridges*. Thesis, University of Michigan.

Parker D.E., Horton B. (2005). *Uncertainties in Central England Temperature 1878-2003 and Some Improvements to the Maximum and Minimum Series*, *Int. J. Climatol.* 25: 1173-1188.

Porker D. E; Legg, T.P; Folland C.K. (1992). *A New Daily Central England Temperature Series, 1772-1991*. *Int. J. Climatol.* 12: 317-342.

Sarveswaran, J; Smith, J.Wand Blockley, D.I. (1998). *Reliability of Corrosion-Damaged Steel Structures using Internal probability Theory*. *Strucural Safety* vol. 20, pp 237-255.

SCOPAC, 2001. *Preparing for the Impacts of Climate Change*, Report Prepared by HalCrow Group Ltd., University of Portsmouth, University of Newcastle and UK Meteorological Office.

SMIC (1971). Inadvertent Climate Modification, USA: MIT Cambridge, Mass.

Smith, K (1975), Principles of Applied Climatology, New York, Mc Graw-Hill.

The Steel Construction Institute (2003), Steel Designers' Manual (6th Ed), Blackwell Science Ltd. Oxford, UK.

Three Regions Climate Change Group, (2008). Your Home in a Changing Climate: Retrofitting Existing Homes for Climate Change Impacts. Greater London Authority.

Tidblad, J; Kucera, V; Mikhailov, A.A; Henriksen, J; Kreislova, K; Yates, T; Stockle, B and Schreiner, M (2001). UN ECE ICP Materials; Dose-Response functions on dry and wet acid deposition effects after 8years of exposure. Water, air and soil pollution 130: 1457-1462.

UIC Code 776-2R. (2009). Design requirements for the rail-bridges based on interaction phenomena between train, track and bridge. 2nd Ed. International Union of Railways.

UK Building Effects Review Group (UKBERG – 1990). The Effect of Acid Deposition on Buildings and Building Materials in the UK, HMSO, London.

Van Engelen, A.F.V; Buisman, J; Ijnsen, F. (2001). A Millenium of weather, winds and water in the low counties. In: Jones, P.D;

Ogilvie A.E.J; Davies, T.D; Briffa, K.R (eds). History and climate: memories of the future? Springer, Heidelberg, pp 101-124.

Wang, J.H.; Wei, F. S; Chang, Y.S; Shih, H.C. (1997).The Corrosion Mechanisms of Carbon Steel and Weathering Steel in SO₂ Polluted Atmospheres. Materials, Chemistry and Physics 47:1-8.

Wellbum, A. (1994), "Air Pollution and Climate Change: The Biological Impact, (2nd Ed) Longman Scientific and Technical, UK, Pg 169.

WMO (1965). A Survey of Human Biometeorology. Technical Note No. 65.

Appendix A

Appendix A1 Definition of Terms

S/N	Definition of Term	Unit
1.	$r_{\text{corrosion}}$ – Corrosion rate of carbon steel	$\mu\text{m/year}$
2.	Time(t)	years
3.	SO ₂ , O ₃ , HNO ₃ , CO ₂ are gaseous pollutants	$\mu\text{g/m}^3$
4.	Temperature (T)	°C
5.	Relative Humidity Rh ₆₀ =Rh-60	%
6.	Amount of precipitation (Rain)	mm
7.	H ⁺ acidic concentration in precipitation	$\mu\text{m/m}^3$
8.	CL ⁻ chloride concentration in precipitation	mg/l
9.	ML is the mass loss	g/m^2
10.	Time of wetness (TOW) is the fraction of time relative humidity > 80% and temperature > 0°C	None
11.	f_{st} is a temperature function, where $f(T)=0.15(T-10)$ when $T<10^\circ\text{C}$, otherwise $f(T)=-0.054(T-10)$	°C
12.	Particulate matter concentration(<10 μm)-PM ₁₀	$\mu\text{m/m}^3$
13.	pH of precipitation	None
14.	ER is erosion rate	$\mu\text{m/year}$

Appendix B

Appendix B1 Estimate of mean values of parameters using Pre-Industrial revolution records

Year	PM ₁₀	SO ₂	NO ₂	O ₃	HN0 ₃	Temp.	pH	RH	Rain	CO ₂
	(μg)m ⁻³					(°C)		(%)	(mm)	ppm
1125	10	5	0.5	20	0.09	9.7	5.5	77	586	279
1175	13	5	0.5	20	0.09	9.8	5.5	77	611	279
1225	16	5	0.5	20	0.09	9.8	5.5	76	604	279
1275	19	5	0.5	20	0.09	9.8	5.5	76	609	279
1325	22	5	0.5	20	0.09	9.7	5.5	76	583	279
1375	14	6	0.5	20	0.09	9.9	5.5	77	577	279
1425	15	6	0.5	20	0.09	9.8	5.5	76	560	279
1475	15	6	0.5	20	0.09	9.8	5.5	76	558	279
1525	15	7	0.5	20	0.09	10	5.5	75	573	279
1575	26	20	4	20	0.24	9.9	5.5	76	549	275
1625	40	40	7	20	0.32	10	5.5	75	549	272
1675	60	120	20	15	0.47	9.8	5.5	75	605	272
Mean	22.08	19.17	2.96	19.58	0.15	9.83	5.50	76.00	580.33	277.50
Variance Standard Dev.	188.74	1022.81	30.19	1.91	0.01	0.01	0.00	0.50	492.56	7.25
Coeff. Of Var.	13.74	31.98	5.49	1.38	0.12	0.09	0.00	0.71	22.19	2.69
	0.62	1.67	1.86	0.07	0.78	0.01	0.00	0.01	0.04	0.01

Appendix B2 Estimate of mean values of parameters using Industrial revolution records

Year	PM ₁₀	S ₀₂	N ₀₂	O ₃	HNO ₃	Temp.	pH	RH	Rain	CO ₂
	(μg)m ⁻³					(°C)		(%)	(mm)	ppm
1675	60	120	20	15	0.47	9.8	5.5	75	605	272
1725	130	260	40	15	0.67	10.4	5.5	75	590	272
1775	140	280	40	15	0.67	10.2	5.5	74	609	277
1825	150	300	50	15	0.75	10.4	5.5	74	605	280
1850	160	320	50	15	0.75	10.4	5.5	74	591	280
1870	190	380	50	15	0.75	10.5	5.5	74	594	280
1890	200	400	58	15	0.81	10.4	5.5	74	557	285
1910	175	350	53	15	0.78	10.6	4.5	74	624	290
1930	160	320	53	15	0.79	10.9	4.5	74	592	295
1950	150	300	60	15	0.84	11.1	4	73	579	305

1970	70	150	75	40	1.52	10.9	4	73	563	321
Mean	144.09	289.09	49.91	17.27	0.80	10.51	5.05	74.00	591.7	287.00
Variance	1776.45	6844.63	173.36	51.65	0.06	0.12	0.38	0.36	354.0	204.91
Standard Deviation	42.15	82.73	13.17	7.19	0.25	0.34	0.62	0.60	18.8	14.31
Coeff. Of Var.	0.29	0.29	0.26	0.42	0.31	0.03	0.12	0.01	0.03	0.05

Appendix B3 Estimate of mean values of parameters using After-Industrial revolution records

Year	PM ₁₀	S _O ₂	N _O ₂	O ₃	HN _O ₃	Temp.	pH	RH	Rain	CO ₂
	(µg)m ⁻³					(°C)		(%)	(mm)	ppm
1970	70	150	75	40	1.52	10.9	4	73	563	321
1990	40	20	75	50	1.73	11.4	5	73	591	352
2010	30	17	40	40	1.15	11.8	5.2	72	582	383
Mean	46.7	62.33	63.33	43.3	1.47	11.37	4.7	73	578.7	352.0
Variance	288.9	3844.2	272.22	22.22	0.06	0.14	0.28	0.2	136.22	640.67
Standard										
Dev.	17.00	62.00	16.50	4.71	0.24	0.37	0.52	0.47	11.67	25.31
Coeff. Of										
Var.	0.36	0.99	0.26	0.11	0.16	0.03	0.11	0.01	0.02	0.07

Appendix B4 Estimate of mean values of parameters using Future projection records

Year	PM ₁₀	SO ₂	NO ₂	O ₃	HNO ₃	Temp.	pH	RH	Rain	CO ₂
	(µg)m ⁻³					(°C)		(%)	(mm)	ppm
2010	30	17	40	40	1.15	11.8	5.2	72	582	383
2030	15	15	20	30	0.71	12.3	5.5	71	590	430
2050	14	14	20	30	0.73	12.9	5.5	71	604	530
2070	13	13	20	30	0.77	14.4	5.5	70	574	610
2090	12	12	20	30	0.73	13.4	5.5	68	551	730
Mean	16.80	14.20	24.00	32.00	0.82	12.96	5.44	70.40	580.20	536.60
Variance	44.56	2.96	64.00	16.00	0.03	0.81	0.01	1.84	311.36	15558.24
Standard Dev.	6.68	1.72	8.00	4.00	0.17	0.90	0.12	1.36	17.65	124.73
Coeff. Of Var.	0.40	0.12	0.33	0.13	0.20	0.07	0.02	0.02	0.03	0.23

**More
Books!** 



yes
I want morebooks!

Buy your books fast and straightforward online - at one of the world's fastest growing online book stores! Environmentally sound due to Print-on-Demand technologies.

Buy your books online at
www.get-morebooks.com

Kaufen Sie Ihre Bücher schnell und unkompliziert online – auf einer der am schnellsten wachsenden Buchhandelsplattformen weltweit!
Dank Print-On-Demand umwelt- und ressourcenschonend produziert.

Bücher schneller online kaufen
www.morebooks.de

OmniScriptum Marketing DEU GmbH
Heinrich-Böcking-Str. 6-8
D - 66121 Saarbrücken
Telefax: +49 681 93 81 567-9

info@omniscrptum.com
www.omniscrptum.com

OMNIScriptum 

